npj | vaccines

Article

Published in partnership with the Sealy Institute for Vaccine Sciences

https://doi.org/10.1038/s41541-024-00940-x

A rationally designed antigen elicits protective antibodies against multiple nosocomial Gram-positive pathogens

Eliza Kramarska[1,6], Eya Toumi[2,6], Flavia Squeglia[1], Diana Laverde[3], Valeria Napolitano[1], Eric Frapy[2], Ida Autiero[1], Oceane Sadones[3], Johannes Huebner[3], David Skurnik[2,4,5] ✉, Felipe Romero-Saavedra[3] ✉ & Rita Berisio[1] ✉

ESKAPE pathogens are responsible for complicated nosocomial infections worldwide and are often resistant to commonly used antibiotics in clinical settings. Among ESKAPE, vancomycin-resistant *Enterococcus faecium* (VREfm) and methicillin-resistant *Staphylococcus aureus* (MRSA) are two important Gram-positive pathogens for which non-antibiotic alternatives are urgently needed. We previously showed that the lipoprotein AdcA of *E. faecium* elicits opsonic and protective antibodies against *E. faecium* and *E. faecalis*. Prompted by our observation, reported here, that AdcA also elicits opsonic antibodies against MRSA and other clinically relevant Gram-positive pathogens, we identified the dominant epitope responsible for AdcA cross-reactive activity and designed a hyper-thermostable and multi-presenting antigen, $Sc(EH)_3$. We demonstrate that antibodies raised against $Sc(EH)_3$ mediate opsonic killing of a wide-spectrum of Gram-positive pathogens, including VREfm and MRSA, and confer protection both in passive and active immunisation models. Our data indicate that $Sc(EH)_3$ is a promising antigen for the development of vaccines against different Gram-positive pathogens.

Enterococci are Gram-positive, facultative anaerobic microorganisms colonising a broad range of hosts, from invertebrates to mammals, including humans[1–3]. When the delicate host bacteria equilibrium is disturbed, Enterococcus sp. can cause life-threatening infections, which are often difficult to treat because of multiple intrinsic and acquired antibiotic resistances. Indeed, enterococci are one of the major nosocomial pathogens[4,5], as they easily infect patients with recent surgery, organ transplantation, diabetes, malignancy, and renal insufficiency[6,7]. *E. faecium* infections have high rates of antibiotic resistance and mortality[8], with more and more strains able to resist to most clinically available antibiotics[9,10]. The World Health Organisation (WHO) has therefore declared vancomycin-resistant *E. faecium* (VREfm) a threat to humankind for which rapid actions are needed[11,12]. Prevention of these infections through vaccines can reduce the usage of antibiotics, and decrease lengths of hospitalisations[13]. Several vaccine antigen candidates against *E. faecium* have been investigated[14–20], but there is so far no vaccine clinically available[21]. Indeed, WHO has broadly categorised bacterial pathogens in four Pipeline Feasibility groups (A-D) in terms of feasibility of vaccine development, based on the progression of vaccine candidates in clinical and preclinical development[22]. In this classification, *E. faecium* belongs to Pipeline Feasibility Group D (low), including "difficult" AMR priority pathogens for which no vaccine candidate has been identified in clinical or preclinical development[22].

Pathogenic bacteria need to hunt for Zn through Zn-binding proteins[23] to be able to survive in the host inhospitable environment and counteract the host-derived Zn limitation[24]. Consistently, mutations in Zn-regulating genes impair virulence and increase susceptibility to the host defence machinery in several bacterial species[25–29]. In *E. faecium*, Zn homoeostasis is regulated by the surface-exposed lipoprotein AdcA, a member of substrate-binding proteins (SBPs) of ATP-binding cassette (ABC) transporters which is upregulated during infection[18]. Similarly, the core genome of *E. faecalis* encodes a conserved AdcACB system and an orphan substrate-binding lipoprotein AdcAII[30]. Inactivation of genes encoding these proteins results in

[1]Institute of Biostructures and Bioimaging, Italian Research Council (CNR), Naples, Italy. [2]CNRS, INSERM, Institut Necker-Enfants Malades, U1151-Equipe 11, Faculté de Médecine, University of Paris City, Paris, France. [3]Division of Paediatric Infectious Disease, Hauner Children's Hospital LMU, LMU Munich, Germany. [4]Department of Clinical Microbiology, Fédération Hospitalo-Universitaire Prématurité (FHU PREMA), Necker-Enfants Malades University Hospital, Assistance Publique-Hôpitaux de Paris, University of Paris City, Paris, France. [5]Division of Infectious Diseases, Department of Medicine, Brigham and Women's Hospital, Harvard Medical School, Boston, MA, 02115, USA. [6]These authors contributed equally: Eliza Kramarska, Eya Toumi.
✉e-mail: david.skurnik@inserm.fr; felipe.romero@med.uni-muenchen.de; rita.berisio@cnr.it

severe growth and survival defects and a decreased resistance to ampicillin, bacitracin, and daptomycin[30]. Analogous Zn uptake mechanisms have been observed in *S. aureus*, which possesses two ABC transporters for Zn acquisition, CntABCDF and AdcABC; whose simultaneous deletion results in growth impairment under Zn-restricted conditions and attenuated virulence[31]. Besides contributing to Zn homoeostasis, AdcA of *S. aureus* was shown to bind human plasminogen and the human negative complement regulator factor H (FH), and thus may support *S. aureus* invasion and colonisation[31]. AdcA of *E. faecium* has been proven to elicit specific, opsonic, and protective antibodies, with extensive cross-reactivity and serotype-independent coverage among the homologous strain *E. faecium* E155 and the clinical isolates *E. faecium* E1162, *E. faecalis* 12030, type 2 and type 5[18]. The observed antigenicity of AdcA lipoprotein, its specific location, and its crucial role in many bacterial species, make AdcA an attractive candidate for vaccine development.

In this study, we used a structural vaccinology approach to develop an AdcA-based vaccine antigen, here denoted as $Sc(EH)_3$, with a cross-reactive potential against several Gram-positive pathogens. To achieve this goal, we designed and computationally validated $Sc(EH)_3$; then, we recombinantly produced the novel molecule and tested it for its properties and efficacy. $Sc(EH)_3$ is a multi-epitope presenting compact protein (of 22 kDa) with exceptional stability to storage and temperature, being highly stable at room temperature. Most important, $Sc(EH)_3$ elicits in rabbits opsonic and protective antibodies that are effective against Gram-positive pathogens, including *E. faecium, E. faecalis* and *S. aureus*.

Results

Anti-AdcA serum mediates Opsonophagocytic killing of different *S. aureus* strains

Given the crucial role of the surface-exposed lipoprotein AdcA in *S. aureus* (which shares with AdcA of *E. faecium* a sequence identity of 66%) and the important challenge of addressing vaccine development against MRSA[32,33], we tested whether antibodies raised against AdcA from *E. faecium* were also able to mediate opsonophagocytosis in three different *S. aureus* strains including MW2, Reynolds and LAC. We chose MW2 and Reynolds strains because they express dominant polysaccharide capsule, CP5 and CP8 respectively, among clinical isolates. Also *S. aureus* USA300 (LAC), which lacks a capsule, is prevalent in the United States[34]. To obtain antibodies, New Zealand rabbits were previously immunised via intramuscular injection with recombinantly expressed AdcA from *E. faecium* and sera containing anti-AdcA antibodies were collected as described (Fig. 1A, B)[18]. In an opsonophagocytic killing assay (OPKA) we observed that anti-AdcA was, indeed, opsonic against all tested *S. aureus* strains, with percentages of opsonophagocytic killing mediated by the anti-AdcA serum in the range 40–60%, compared with 0–20% killing of the pre-immune sera (Fig. 1C–E). To assess whether antibodies that mediate the opsonic killing of *S. aureus* are specific towards AdcA, we incubated the anti-AdcA sera with different amounts of recombinant AdcA (opsonophagocytic killing inhibition assay, OPIA)(Fig. 1F, G). As shown in Fig. 1G, the opsonophagocytic killing of *S. aureus* MW2 mediated by the anti-AdcA serum was inhibited in a dose-dependent manner by the purified AdcA of *E. faecium*.

Structure-based identification of AdcA epitope

The observed cross-reactivity of *E. faecium* AdcA sera binding to both *E. faecium* and *S. aureus*, prompted us to investigate the molecular determinants responsible for antigenicity of this protein. As shown in Fig. 2A, three distinct regions can be identified in the AdcA (protein ID: WP_002297324.1) sequence: a signal peptide at the N-terminus, a periplasmic Zinc-uptake complex component A (ZnuA) and a lipocalin-like zinc-recruitment domain (ZinT), as detected by sequence analysis in the PFAM (Protein Families Database) database[35] (Fig. 2A). As a first step for structure-based epitope identification approach, we homology modelled the structure of AdcA, using the programme MODELLER[36] after consensus-based sequence alignment with HHPred[37] (Fig. 2). In AdcA homology model, the N-terminal ZnuA domain and the C-terminal ZinT domain are connected by a long loop region, embedded between residues 314–330 (Fig. 2A, B). The ZnuA domain is formed by two lobes adopting (β/α)4 folds and connected by a long α−helix (residues 169–199), whereas the ZinT domain adopts an 8-stranded β-barrel structure terminating with a helical region of four short helices (Fig. 2B). Each domain presents a cluster of His-residues which is putatively involved in Zn binding (Fig. 2B). Consistently, they were both shown to bind Zn in the homologue of AdcA from *S. pneumoniae*; albeit being the ZnuA domain necessary and sufficient for Zn acquisition[38].

Preliminary sequence-based B-cell epitope prediction, using Bepipred3[39], identified the strongest immunogenic regions on the ZnuA domain (Fig. 2C). Structure-based epitope prediction using Discotope-2.0[40] (Fig. 2C) and ElliPro[41] confirmed this region as the most immunogenic of the AdcA structure. The best-predicted antigen is located on a large and flexible loop between α4 and β4 secondary structure elements of the ZnuA domain, between residues G125-E141 (Fig. 2D). Antigenicity, allergenicity, and toxicity, further analysed with VaxiJen v2.0[42], AllerTop 2.0/AllergenFP1.0[43,44], ToxinPred[45], showed that the best epitope 125-GSEEEDHDHGEEDHHHE-141 is also predicted to be non-allergenic and non-toxic (Table 1). Due to the abundance of glutamic acid (E) and histidine (H) in this loop sequence, we denoted it as EH-motif (Fig. 2D).

The EH-motif sequence reacts with anti-AdcA antibodies and partially inhibits the opsonic killing elicited by the anti-AdcA serum

Prompted by the bioinformatic prediction of the EH-motif as a dominant epitope, we tested whether antibodies raised against AdcA were able to bind this specific peptide sequence. To this end, we obtained two synthetic versions of the epitope, one with biotinylation in the N-terminal part of the peptide designated N-biot-EH (K(Biot)GSEEEDHDHGEEDHHHE) and one with biotinylation in the C-terminal part of the peptide designated C-biot-EH (GSEEEDHDHGEEDHHHEK(Biot)). Both peptides were applied to streptavidin-coated ELISA plates. As shown in Fig. 3A, both peptides were recognised by the antibodies raised against full-length recombinant AdcA, with C-biot-EH showing a higher affinity for the anti-AdcA serum, compared with the N-biot-EH (Fig. 3A). Therefore, we tested if these peptides were able to inhibit the opsonic killing mediated by anti-AdcA antibodies against both *E. faecium* and *S. aureus*. To assess selectivity of antibodies, we performed OPIA experiments, where we preincubated the anti-AdcA serum with either C-biot-EH and N-biot-EH peptides and with the two positive controls, the full length recombinant AdcA and the ZnuA domain. We observed that both peptides were able to inhibit the opsonic activity of the anti-AdcA antibodies against the *S. aureus* MW2 (Fig. 3B–E) and *E. faecium* 11236/1 (Fig. 3F–I) in a concentration dependent manner. As expected, the observed inhibition of opsonic killing due to EH-peptides was lower than that observed for the full-length AdcA protein, since the tested serum was originally raised against full-length AdcA.

The best AdcA epitope, the EH-motif, is highly conserved among multiple species and suitable as a cross-reactive antigenic sequence

To design a broadly cross-reactive antigen, we performed a thorough sequence analysis to evaluate the level of antigen conservation among different strains of *Enterococcus* sp, and among different pathogenic bacteria from the WHO list. Sequence dataset collection and the following alignment were performed using BlastP[46] and Clustal Omega EMBL-EBI[47] software, respectively.

First, we searched homologues of the ZnuA domain of AdcA among multiple bacterial species. Using a sequence identity (seqid) threshold of 60%, we identified 157 sequences in *E. faecium* isolates (taxid: 1352), and further 318 sequences in *Enterococcus* sp. (taxid: 1350). Based on the promiscuity of ZnuA-like domains of Zn-acquiring proteins in *Enterococcus* sp., we decided to broaden our investigation to include closely related

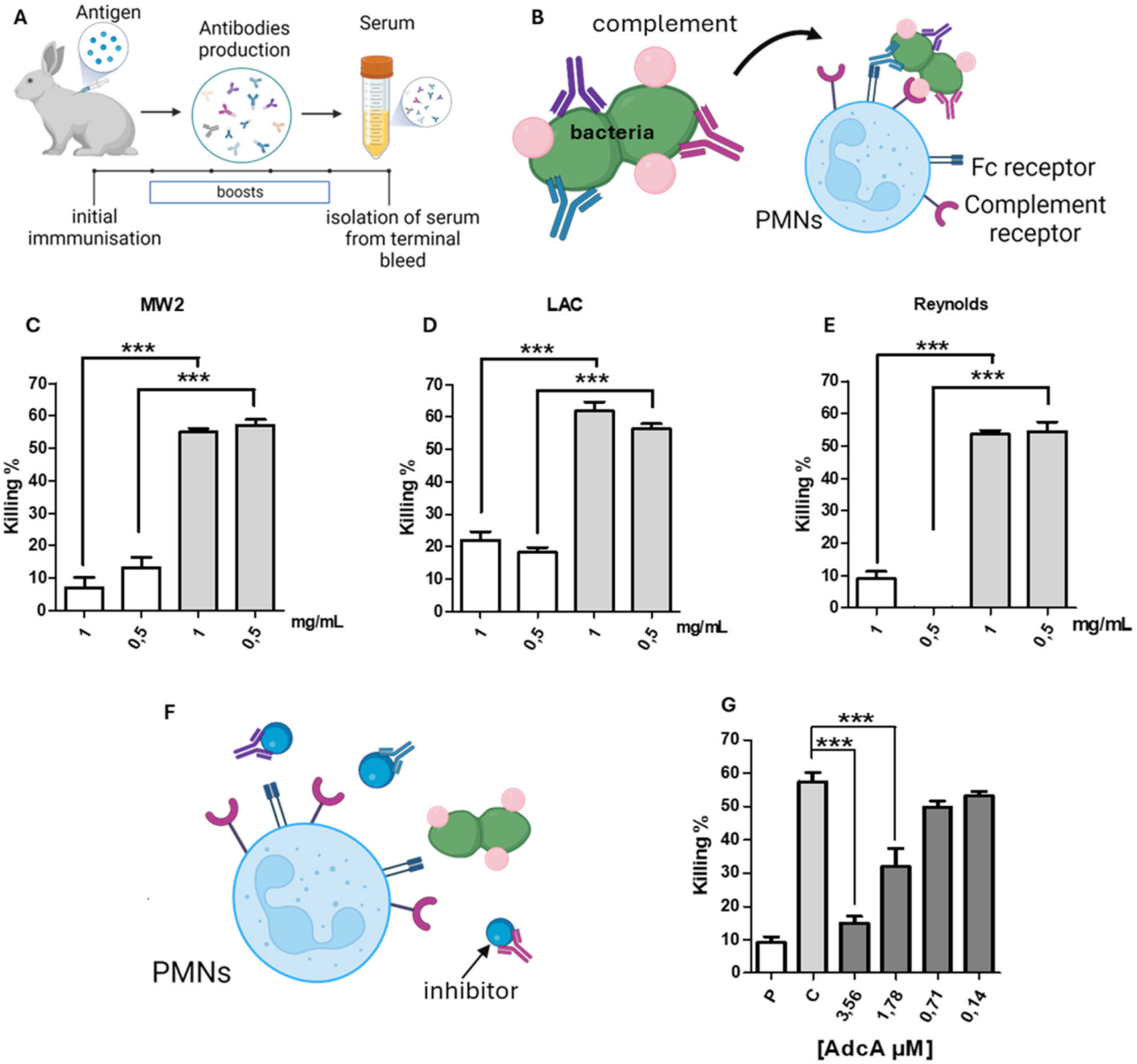

Fig. 1 | Opsonophagocytic killing activity (OPKA) of anti-AdcA serum against different *S. aureus* strains. A schematic representation of rabbit immunization (**A**) and mechanism of OPKA (**B**). Antigen-specific antibodies and complement proteins opsonise bacteria and facilitate the uptake of the antibody-bacteria complex by phagocytes (PMN). **C** OPKA against *S. aureus* strains MW2, (**D**) LAC, and (**E**) Reynolds were tested with sera raised against the recombinant AdcA from *E. faecium*, used at total IgG concentrations ranging from 1 to 0.5 mg/mL (grey bars). The effectiveness of opsonophagocytic killing by the anti-AdcA rabbit sera (MW2 - C, LAC – D, and Reynolds - E) was compared to that by the pre-immune rabbit sera (white bars). Statistical significance was tested by the unpaired two-tailed *T* test with a 95% confidence interval with a Bonferroni post hoc test using pre-immune and terminal immune sera at the same concentration. Bars and whiskers denote mean values ± standard errors of the mean of replicates within one assay. $^{*}P \leq 0.025$, $^{**}P \leq 001$, $^{***}P \leq 0.001$. **F** Schematic representation of an OPIA assay. Antibodies, once engaged by their antigens (inhibitors) are unable to opsonise, leading to a decrease in bacterial killing. **G** OPIA of anti-AdcA rabbit serum performed by incubation of serum with recombinant AdcA protein and tested against *S. aureus* MW2. Antibodies raised against the AdcA at 0,5 mg/mL of total IgG concentration were pre-incubated with different amounts of AdcA (black bars) in a range from 0.14 to 3.56 µM. Pre-immune serum (P) at 0,5 mg/mL of total IgG concentration was used as a negative control, and anti-AdcA sera (**C**) without incubation with AdcA, at 0.5 mg/mL of total IgG concentration was used as a positive control. Statistical significance of inhibition was performed by the One-way analysis of variances test, followed by the Dunnett's multiple comparison post hoc test. Bars and whiskers denote mean values ± standard errors of the mean of replicates within one assay. $^{*}P \leq 0.05$, $^{**}P \leq 0.01$, $^{***}P \leq 0.001$.

Streptococcus sp. (taxid: 1301), where we identified 549 homologous sequences. The same analysis conducted on ZnuA domains of *S. aureus* (taxid: 1280) showed that a lower albeit significant sequence identity with ZnuA of *E. faecium* AdcA. By lowering the seqid threshold to 30%, a value that still identifies similar structural folds, we could detect 627 sequences in *S. aureus* (Supplementary data 1–4).

Using the sequence sets obtained for each bacterial isolate, we then checked the intra-species conservation of the EH-motif. In *E. faecium*, the seqid of the EH-motif is 80% when computed on all 157 sequences, of which 89 sequences present an almost fully conserved EH-motif (seqid 99%, Fig. 4). Almost all ZnuA sequences of *Enterococcus* sp. (303 out of 318) present an EH-motif with small or no variations (sequence identity 87%, Fig. 4), indicating strong conservation of the EH-motif also in clinically relevant *E. faecalis* isolates. In *Streptococcus* sp., 548 out of 549 sequences had a highly conserved EH-motif (seqid 81%, Fig. 4). Interestingly, 404 out of 627 sequences with seqid 30%

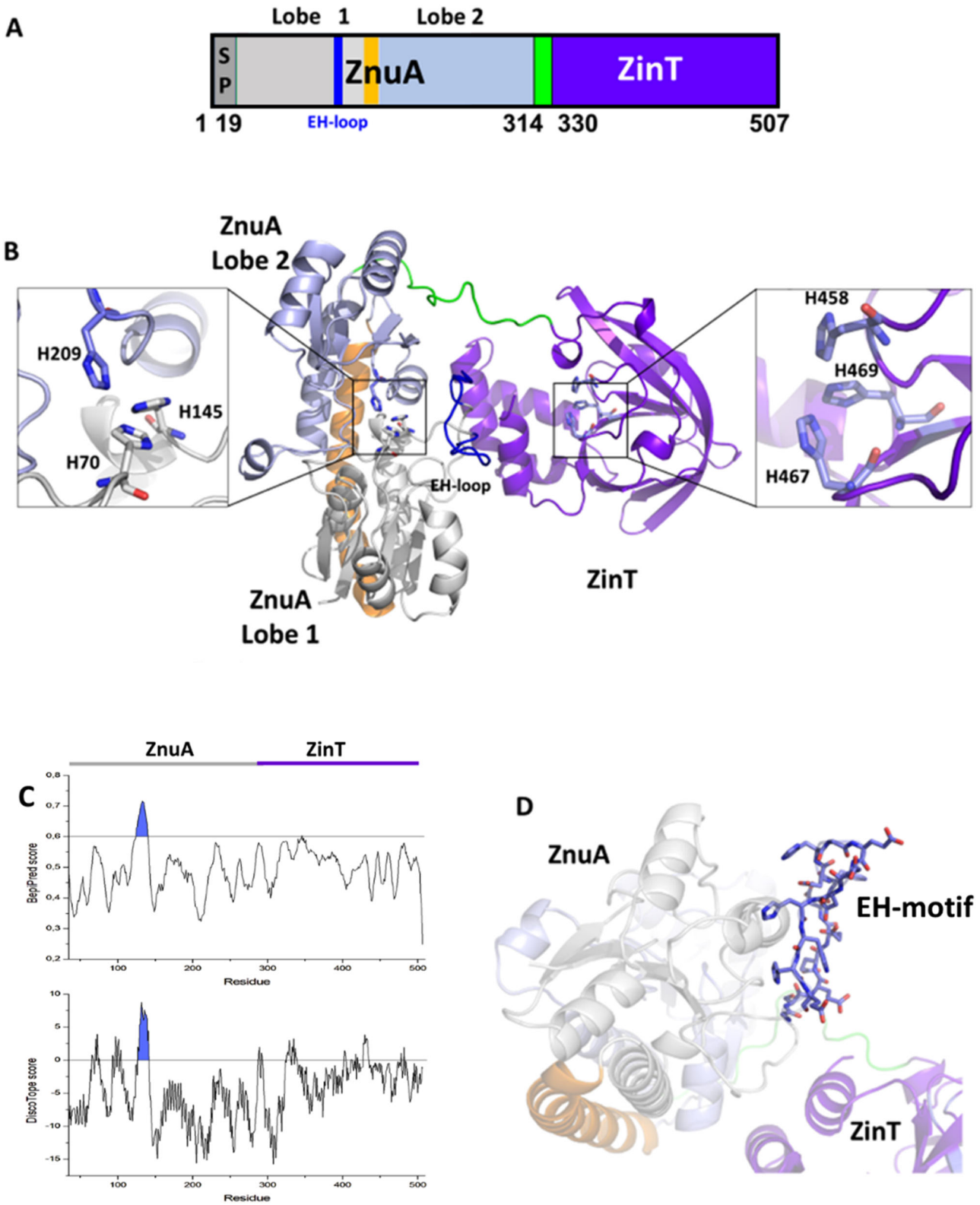

Fig. 2 | Structural information on AdcA from *E. faecium* and epitope identification. A Domain composition of AdcA based on PFAM analysis. **B** Cartoon representation of the homology model of full-length AdcA, computed with MODELLER using the structure of AdcA from S. pneumoniae (PDB code: 7jj9, sequence identity 65%) as a template. The ZnuA domain, formed by Lobe 1 (light grey) and Lobe 2 (light blue) is connected to the ZinT domain (violet) through a loop, represented in green. The two zoom panels report putative Zn-binding histidines, represented in stick, in each domain. **C** Epitope prediction using BepiPred (top) and Discotope (bottom); the region with highest score is coloured blue. **D** Cartoon and stick representation of the most antigenic region, here named as EH-motif, located in Lobe 1 of the ZnuA domain.

Table 1 | Prediction of the antigenicity, allergenicity, and toxicity of AcdA portions

	VaxiJen score	AllerTop 2.0	AllergenFP 1.0	ToxinPred
AdcA	0.55	Non-allergen	Non-allergen	Non-toxic
ZnuA	0.46	Non-allergen	Non-allergen	Non-toxic
ZinT	0.69	Likely allergen	Non-allergen	Non-toxic
EH-motif	1.59	Non-allergen	Non-allergen	Non-toxic

VaxiJen threshold for antigenicity is set to 0.4.

identified for *S. aureus*, embed a highly conserved EH-motif (seqid 97.5%, Fig. 4). These sequences contain the *S. aureus* strains MW2, LAC and Reynolds, for which we have experimentally proven an opsonic activity of anti-AdcA antibodies (Fig. 1).

To evaluate the inter-species conservation of the EH-motif belonging to *E. faecium* AdcA, we computed the consensus sequence of each species, using the Jalview[48], and then aligned this consensus with the sequence of AcdA EH-motif. As shown in Fig. 4B, the EH-motif sequence shares 100% seqid with the consensus computed for *E. faecium*, consistent with the high conservation of this motif in *E. faecium* family. Almost full conservation of the EH-motif is also observed with the consensus sequence of streptococci (seqid 93.3%), Fig. 4B. Lower sequence identities, still higher than 60%, are observed with *S. aureus* (Fig. 4B). Full datasets, a list of bacteria and alignments are available in supplementary data. These data predict a good efficacy of the EH-motif sequence as an antigen not only against multiple *E. faecium* strains, but against all the described bacterial species.

Design of a hyper-stable, multi-presenting, and cross-reactive scaffolded antigen

Once we had established that the EH-motif is strongly immunogenic and promiscuous among different pathogens, we focused on designing a hyper stable protein embedding multiple copies of this peptide antigen. As a vehiculating molecule, we chose the domain D1 (residues 1-210, PDB code 6gpc) of the highly stable arginine binding protein (ArgBP) from *T. maritima* (PDB code 4prs) The rationale for the choice of this domain as an accepting scaffold for the antigenic EH-motifs mainly relies on its extraordinary stability to temperature and chemical denaturants[49], also when dissected from the entire protein[50], a characteristic that allows structural manipulations albeit preserving the protein conformational stability. Also, the D1 domain of ArgBP presents more loops to host the antigenic motifs, thus potentially acting as a multi-antigen presenting molecule. Molecular modelling sessions were performed to identify the proper locations of the EH-motif to prevent the destabilisation of the protein structure. The D1 domain has a compact α/β fold, whose main body is formed by 5 α helices surrounding a central β sheet. The structure contains two β-hairpin motifs protruding from the main fold and embedding loop regions between Asp26 and Asn70 and between Ala95 and Glu102 (Supplementary Fig. 1). Due to their flexibility and outward protrusion, we identified these loops as more amenable for antigen insertion, without inducing protein distortions (Supplementary Fig. 1). Therefore, we designed a chimeric protein with the D1 domain as accepting scaffold (Sc) and the EH-motif between E27 and N28, G97 and G98 and at the N-terminal side of the protein (Fig. 5A, Supplementary Table 1), here designated as $Sc(EH)_3$. The obtained model was used for molecular dynamics (MD)[51]. DiscoTope analysis[52] on the minimised model shows that the sole predicted antigenic regions of $Sc(EH)_3$ are the inserted EH-motifs (Fig. 5B, Supplementary Fig. 1).

MD dynamics was used to validate the computationally designed model through the analysis of its structural and dynamic features. MD outcomes are generally important for model quality estimation, an important and propaedeutic step to experimental work[53]. We run three MD trajectories, each of 500 ns, with different starting velocities to improve the conformational ensemble search and extensively explore the dynamic features of the protein upon insertion of EH-motifs. The root-mean-square deviation (RMSD) profiles of $Sc(EH)_3$, computed on Cα atoms with the respect to the starting model, suggests that the simulated system consistently reaches an equilibrium phase in about 100 ns in the three parallel runs, showing comparable mean and standard deviations of RMSD values (Supplementary Fig. 2). To dissect conformational changes of the accepting scaffold from those of the inserted EH-motifs, we computed RMSD values of these isolated protein core and inserted EH-motifs (Fig. 5C). It appears clear that $Sc(EH)_3$ presents as a compact and stable core with low and stable RMSD values, whereas the EH-motifs show large conformational variations (Fig. 5C). The high dynamic nature of EH-motifs is also confirmed by the root mean squared fluctuations (RMSF) of the relative residues (Fig. 5D), which show values in the range from 5 to 15 Å, while the RMSF of all other residues remains below 5 Å. The MD analyses suggest that the EH-motifs are a region of peculiar flexibility, whereas the stability of the protein core region is well preserved, with no distortion in the connecting regions. The high flexibility in antigenic sites is a good premise, since flexible epitopes can elicit a diverse antibody response through their conformational adaptation during the binding event to multiple antibodies[54]. After validation of $Sc(EH)_3$ model, we sub-cloned the synthetic gene encoding for its amino acid sequence into pETM-13, expressed and purified in high yields, as monitored by SDS-PAGE electrophoresis. Light Scattering studies confirmed that $Sc(EH)_3$ is a monomer in solution, with a weight-average molar mass of 22.0 ± 0.1 kDa (Supplementary Fig. 3A). Of note for vaccine development, $Sc(EH)_3$ is extremely thermo-resistant and long-term stable at 37 °C. Indeed, circular dichroism (CD) spectroscopy shows a fully conserved spectrum of the protein after 1 h incubation at 37 °C, compared to that at 20 °C (Fig. 5E). Also, $Sc(EH)_3$ is still endowed with a secondary structure content after incubation at 100 °C (Fig. 5E). Consistently, thermal unfolding, analysed by recording the CD signal at 222 nm, shows that the denaturation transition is not complete at 100 °C (Fig. 5F). Full unfolding could be achieved in the temperature range 20–100 °C only in the presence of a chemical denaturant, specifically 3 M guanidine hydrochloride (GuHCl), with a melting temperature (Tm) of 52 °C (Fig. 5F). As shown in Fig. 5G, $Sc(EH)_3$ is also highly resistant to proteolysis, as it can be stored for at least 30 days at 37 °C with no sign of degradation. In the same conditions, AdcA exhibits a visible degradation pattern, with the accumulation of two major degradation bands in the SDS-PAGE gels (Fig. 5G, Supplementary Fig. 3B, C).

$Sc(EH)_3$ elicits antibodies that generate strong and specific opsonic killing against *E. faecium*, *S. aureus* and *E. faecalis*

The $Sc(EH)_3$ protein was used to immunise two female New Zealand white rabbits, which were exsanguinated two weeks after the last injection (see "Methods"). To generate a serum that represents an average immune response, the terminal bleeds of both rabbits were mixed in equal volumes, generating the anti-$Sc(EH)_3$ serum. The same procedure was applied to the pre-immune sera, used as a negative control. As a preliminary test, we evaluated the ability of the anti-$Sc(EH)_3$ antibodies to specifically recognise C-biot-EH by ELISA. We found that the anti-$Sc(EH)_3$ could specifically bind to the epitope up to a dilution of 1:4000 whereas the pre-$Sc(EH)_3$ did not show any binding at dilutions as high as 1:250 (data not shown). This confirmed that the anti-$Sc(EH)_3$ serum contained antibodies directed against the EH-motif. We then used OPKA to test if the anti-$Sc(EH)_3$ antibodies can mediate opsonic killing of *E. faecium* 11236/1, *S. aureus* MW2 and *E. faecalis* T2. As shown in Fig. 6A, the anti-$Sc(EH)_3$ serum antibodies, in a concentration of 0.4 mg/mL, were significantly better at inducing opsonophagocytic-dependent *E. faecium 11236/1* killing, compared to anti-AdcA sera. We observed an average opsonic killing of 67% at 0.4 mg/mL IgG dilution, compared to 46% of sera raised against full-length AdcA. Importantly, $Sc(EH)_3$ was also able to induce opsonic killing of *S. aureus* MW2 (Fig. 6B) and *E. faecalis* T2 (Fig. 6C). In the case of *S. aureus* MW2, significantly higher killing activity than anti-AdcA was observed in particular at lower concentrations of anti-$Sc(EH)_3$ sera, with 48% killing of

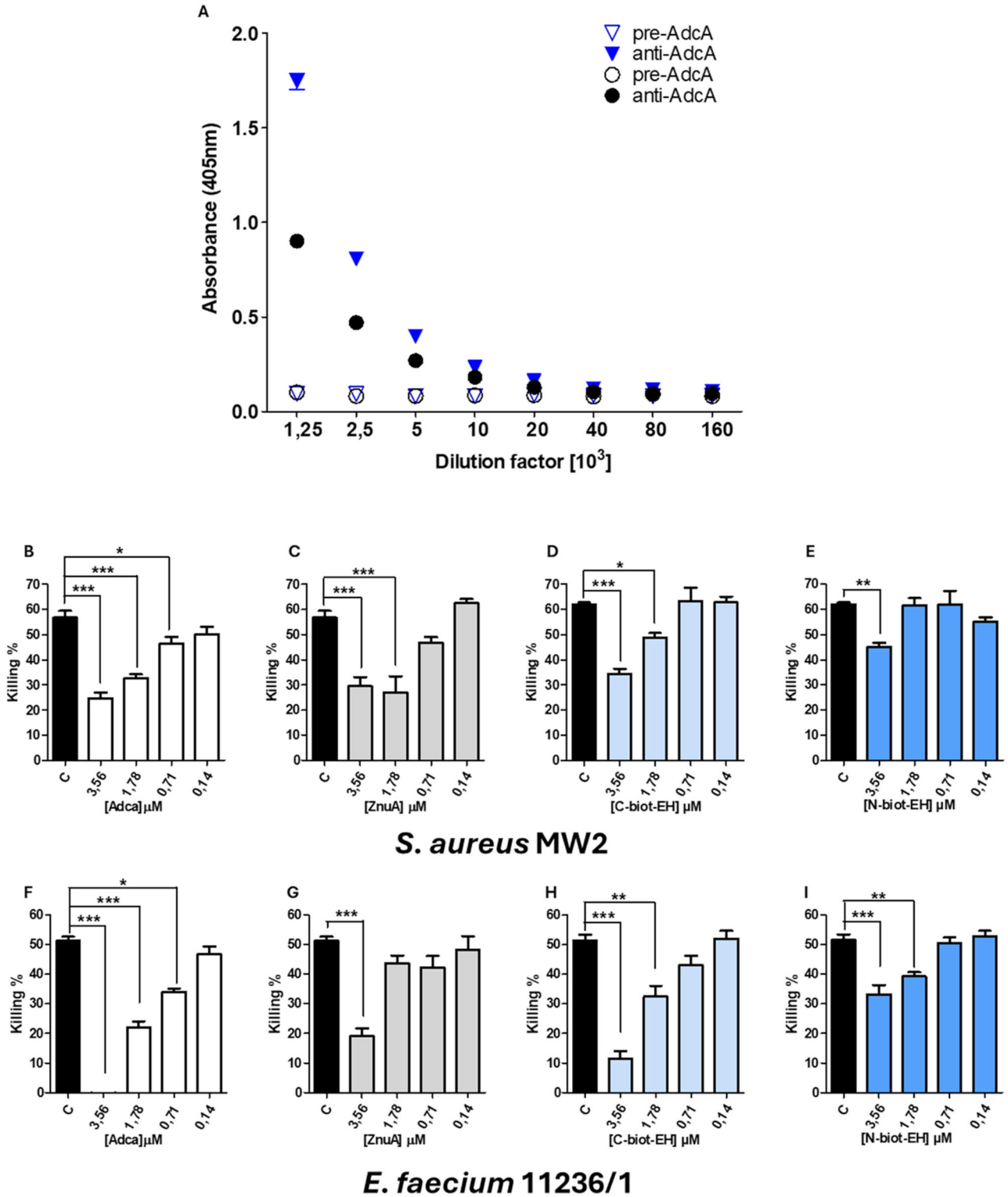

Fig. 3 | The EH-motif is recognised by antibodies raised against full-length recombinant AdcA and inhibit the opsonic killing mediated by anti-AdcA antibodies against both *E. faecium* and *S. aureus*. **A** Immuno-reactivity towards the EH-peptides detected by enzyme-linked immunosorbent assays (ELISA). Either the N-biot-EH (black) or C-biot-EH (blue) were added to streptavidin coated plates and tested by ELISA with pre-AdcA or anti-AdcA sera. **B**–**E** Inhibition of opsonophagocytic killing activity of anti-AdcA 0.5 mg/mL of total IgG concentration rabbit serum against *S. aureus* MW2 and (**F**-**I**) *E. faecium* 11236/1 by addition of EH-peptides. Antibodies raised against the recombinant AdcA were pre-incubated with the different inhibitors (in the concentration range 0.14 to 3.56 µM), including recombinant AdcA (white), ZnuA domain (grey), C-biot-EH (light blue) or N-biot-EH (blue). As positive control (**C**) we used sera anti-AdcA 0.5 mg/mL of total IgG concentration with no inhibitor (black). Names of tested strains are visible below corresponding assays. Statistical significance was computed by the One-way analysis of variances test, followed by the Dunnett's multiple comparison post hoc test. Bars and whiskers denote mean values ± standard errors of the mean of replicates within one assay. $^{*}P \leq 0.05$, $^{**}P \leq 0.01$, $^{***}P \leq 0.001$.

A

Bacteria	Treshold	Number of sequences	Consensus sequence with percentage of single amino acid conservation in predicted EH-loop	Average conservation of EH-loop
Enterococcus faecium	60%	89		99%
Enterococcus sp.	60%	303		87%
Streptococcus sp.	60%	548	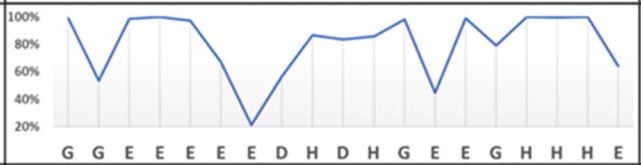	81%
Staphylococcus aureus	30%	404		97,5%

B

Bacteria	Parwise alignment of consensus sequences with AdcAfm EH-loop using Lalign	Sequence identity
Enterococcus faecium	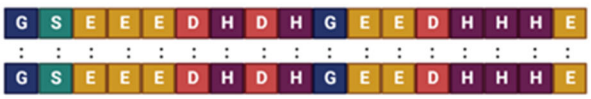	100%
Enterococcus sp.		61,9%
Streptococcus sp.		93,3%
Staphylococcus aureus		64,3%

Fig. 4 | The EH-motif is conserved in a wide spectrum of Gram-positive bacteria. Computational analysis of (**A**) EH-motif conservation in different bacterial species, and (**B**) pairwise alignment of consensus sequences of each dataset in (**A**) with the EH-motif of AdcA of *E. faecium*. Only regions with the highest Waterman-Eggert score are shown (computed with Lalign).

anti-Sc(EH)$_3$ at 0.2 mg/mL compared to 32% in the case of anti-AdcA. Even at 0.05 mg/mL, anti-Sc(EH)$_3$ sera were significantly more effective (21% killing), compared anti-AdcA sera (6% killing) (Fig. 6B). As for *E. faecalis* T2, sera raised by both AdcA and Sc(EH)$_3$ were able to kill *E. faecalis* T2, with a maximum killing of about 70% at the maximum antibody concentration of 0.4 mg/mL (Fig. 6C). Higher killing was induced by anti-Sc(EH)$_3$ compared to anti-AdcA at lower antibody concentration (44% compared to 30% at 0.2 mg/mL) (Fig. 6C). These data prove that both AdcA and Sc(EH)$_3$ act as cross-reactive antigens. However, Sc(EH)$_3$ elicits antibodies that generate the strongest opsonic killing against all tested Gram positive bacteria.

To verify the specificity of opsonising antibodies against the EH-motifs of Sc(EH)$_3$, opsonophagocytic inhibition assays were carried out by pre-incubating the anti-Sc(EH)$_3$ sera with different inhibitors at different

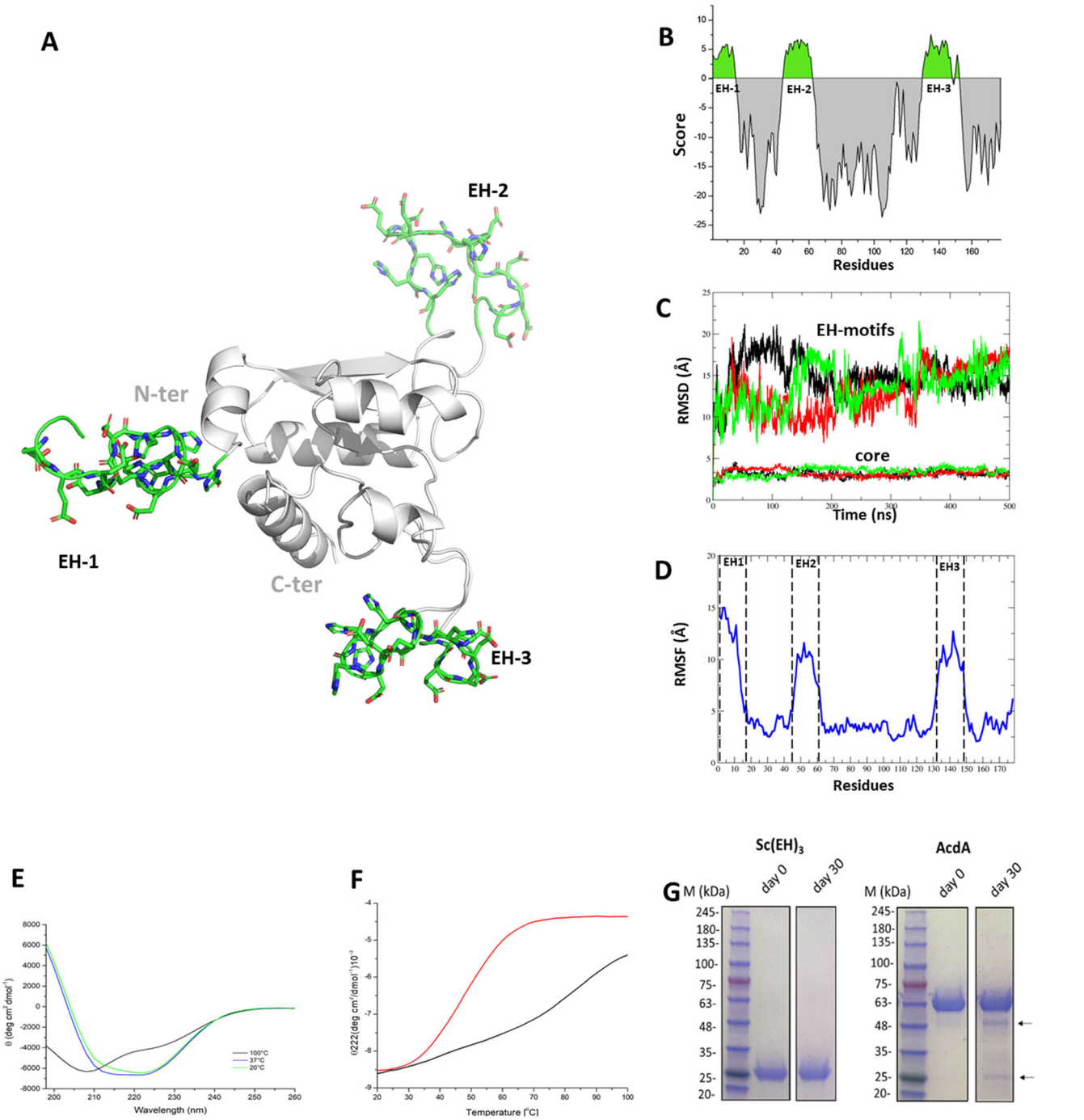

Fig. 5 | Design, validation, production and characterisation of a hyper stable multi-presenting antigen. A Molecular model of $Sc(EH)_3$ after energy minimisation. **B** DiscoTope predictions of $Sc(EH)_3$, showing predicted antigenicity solely for the inserted EH-motifs. **C** Root-mean-square deviations (RMSD) computed on Cα atoms, reported for either the core or the EH-motifs residues for the three MD simulations at three increasing velocities in black, red, and green. **D** Root-mean-square fluctuations (RMSF) on Cα atoms showing high flexibility solely for the three EH-motifs. **E** Far-UV CD spectra were measured at 0.2 mg mL^{-1} in 20 mM sodium phosphate buffer (pH 7.4) after incubation for 1 h at 20 °C (green), 37 °C (blue) and 100 °C (black). **F** Thermal denaturation curves of $Sc(EH)_3$ monitored at 222 nm in 20 mM sodium phosphate buffer (black) and in the presence of 3 M GuHCl denaturant (red). **G** Resistance to storage at 37 °C for 30 days of $Sc(EH)_3$ compared to AdcA, as shown by SDS-gel electrophoresis. Degradation bands of AdcA are highlighted by arrows.

concentrations, including $Sc(EH)_3$, AdcA, or ZnuA. Anti-AdcA sera incubated with AdcA protein were used as a control (Fig. 6D–F). In all cases, we observed a concentration dependent reduction of killing induced by sera, indicating specificity of antibodies against each added antigen. Specifically, for *E. faecium* 11236/1 we observed a reduction in the killing of anti-$Sc(EH)_3$ antibodies, at the maximum concentration used, by 54%, 41%, and 53% upon incubation with AdcA, ZnuA, and $Sc(EH)_3$, respectively (Fig. 6D). In the case of *S. aureus* MW2, killing reduction at the highest inhibitor concentration was 49%, 51%, and 65% for AdcA, ZnuA and $Sc(EH)_3$, respectively (Fig. 6E). Similar OPIA results were obtained for *E. faecalis* T2, showing that sera-mediated killing was significantly inhibited by all proteins in a concentration dependent manner (Fig. 6F), thus confirming the specific recognition of antibodies for the EH-motif, which is common to all inhibitors.

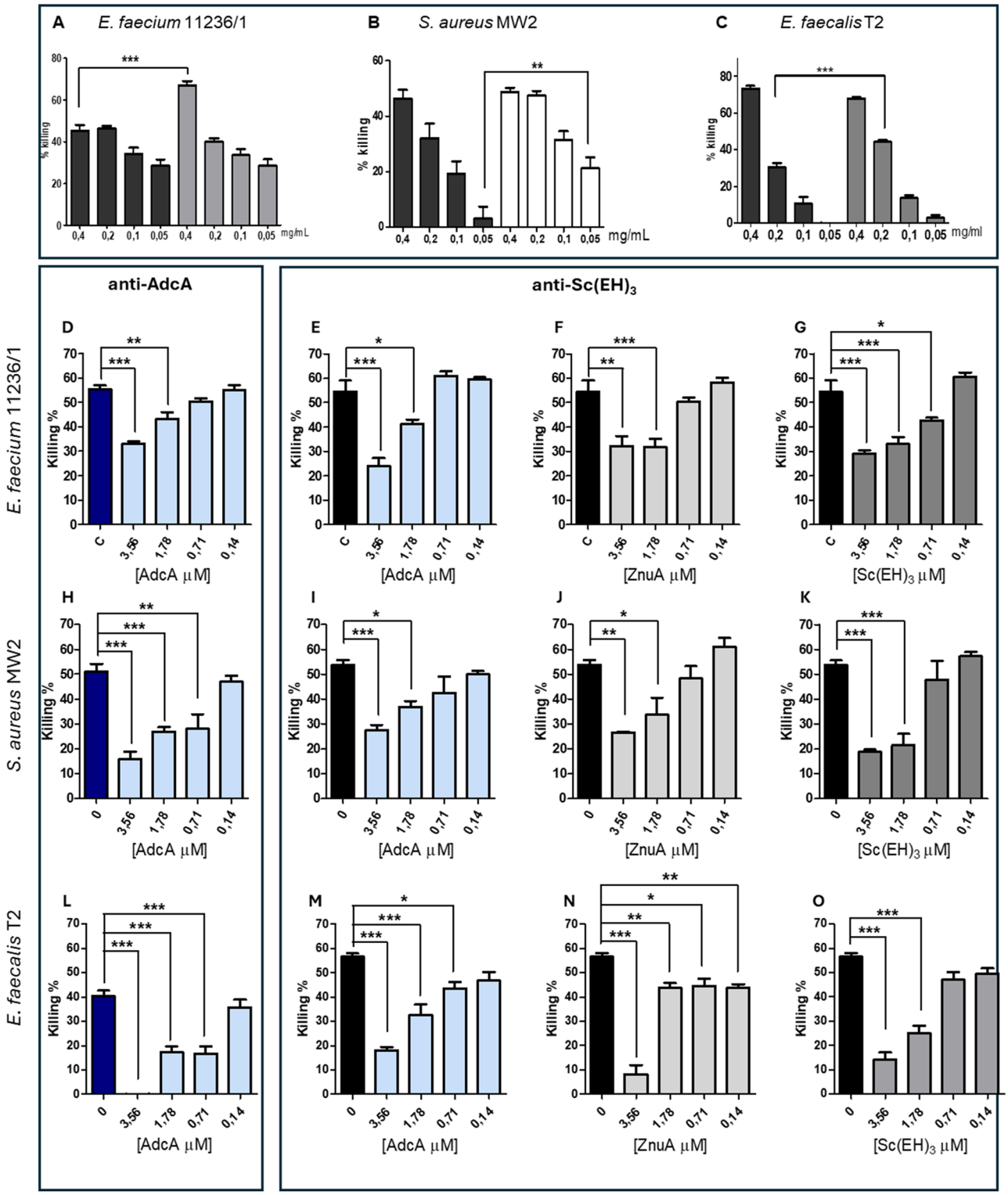

Fig. 6 | OPKA and OPIA assays against *E. faecium* 11236/1, *S.aureus* MW2 and *E. faecalis* T2. OPKA assays against (**A**) *E. faecium* 11236/1, (**B**) *S. aureus* MW2, and (**C**) *E. faecalis* T2. OPKA killing percentages mediated by anti-Sc(EH)$_3$ sera are compared to those mediated by anti-AdcA (black bars). The statistical significance was tested by the unpaired two-tailed *T* test with a 95% confidence interval with a Bonferroni post hoc test using anti-AdcA and anti-Sc(EH)$_3$ sera at the same concentration. Bars and whiskers denote mean values ± standard errors of the mean. $^{*}P \le 0.0125$, $^{**}P \le 0.01$, $^{***}P \le 0.001$. OPIA assays with 0.4 mg/mL anti-AdcA or anti-Sc(EH)$_3$ sera against *E. faecium* 11236/1 (**D**–**G**) *S. aureus* MW2 (**H**–**K**) and *E. faecalis* T2 (**L**–**O**) by addition of different inhibitors. Anti-AdcA and anti-Sc(EH)$_3$ were pre-incubated with different concentrations of inhibitors, including recombinant AdcA (light blue bars), ZnuA domain (light grey bars), and recombinant Sc(EH)$_3$ (dark grey bars). Anti-AdcA sera incubated with AdcA were used as positive controls (**D**, **H**, **L**). As negative controls (0) for each plot, we used sera at 0.4 mg/mL anti-AdcA (dark blue bar) and anti-Sc(EH)$_3$ (black bars) without inhibitors. Statistical significance of inhibition was performed by the One way analysis of variances test, followed by the Dunnett's multiple comparison post hoc test. Bars and whiskers denote mean values ± standard errors of the mean of replicates within one assay. $^{*}P \le 0.05$, $^{**}P \le 0.01$, $^{***}P \le 0.001$.

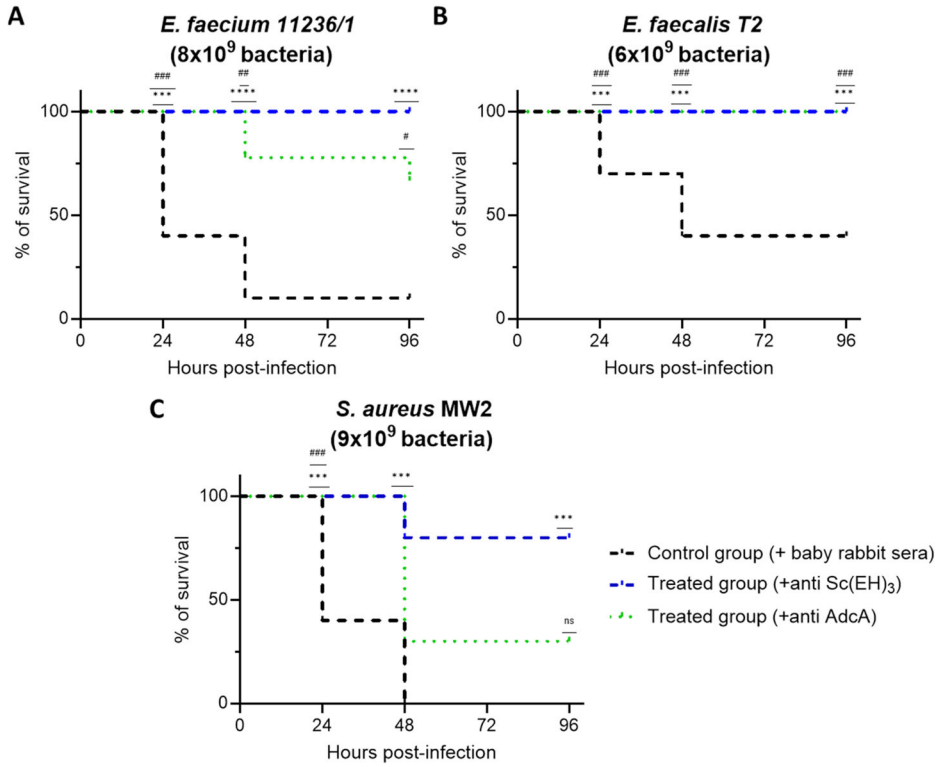

Fig. 7 | In vivo passive protective efficacy of anti-Sc (EH)$_3$ and anti-AdcA polyclonal antibodies against *E. faecium* 11236/1, *E. faecalis* T2 and *S. aureus* MW2. **A** The percentage of survival mice during the protection assay against 8×10^9 CFU of *E. faecium* 11236/1. The discontinuous blue line represents the group treated with the anti-Sc (EH)3 antibody ($n = 10$), the discontinuous green line represents the group treated with the anti-AdcA antibody ($n = 10$) and the discontinuous black line represents the negative control group with mice receiving inactivated baby rabbit sera (BRS) ($n = 10$). **B** The percentage of survival mice during the protection assay against 6×10^9 CFU of *E. faecalis T2*. The discontinuous blue line represents the group treated with the anti-Sc (EH)3 antibody ($n = 10$), the discontinuous green line represents the group treated with the anti-AdcA antibody ($n = 10$) and the discontinuous black line represents the negative control group with mice receiving inactivated baby rabbit sera (BRS) ($n = 10$). **C** The percentage of survival mice during the protection assay against 9×10^9 CFU of *S. aureus* MW2. The discontinuous blue line represents the group treated with the anti-Sc (EH)3 ($n = 10$), the discontinuous green line represents the group treated with the anti-AdcA ($n = 10$) and the discontinuous black line represents the negative control group with mice receiving inactivated baby rabbit sera (BRS) ($n = 10$). Statistical differences between groups were assessed using Log Rank (Mantel-cox test). Difference between the treated groups with anti-Sc (EH)3 antibody and the control groups are marked by star symbol, ns: not significant; *$p < 0.05$, **$p < 0.01$, ***$p < 0.001$ and ****$p < 0.0001$. Difference between the treated groups with anti-AdcA antibody and the control groups are marked by hash symbol, ns: not significant; #: $p < 0.05$, # #: $p < 0.01$, # # #: $p < 0.001$ and # # # #: $p < 0.0001$.

Estimation of the LD50 of the different used strain on Balb/C mice. To determine the lethal dose of each strain, different bacterial concentrations were injected into mice and the mortality rate was recorded for each group. We defined an approximate LD50 around 5×10^9 CFU for each bacterium since we recorded 50% of mortality between 3×10^9 and 6×10^9 CFU (Supplementary Table 2).

Anti-Sc(EH)3 and anti-AdcA antibodies are protective in mouse infection models

To determine whether anti-Sc (EH)$_3$ and the anti-AdcA antibodies confer protection to mice against Gram-positive bacterial infections due to bacterial strains *E. faecium 11236/1*, *faecalis T2*, and *S. aureus* MW2, mice were passively immunised in a lethal bacteremia mouse model (Supplementary Fig. 4). As shown in Fig. 7A, after 96 h of bacterial challenge with 8×10^9 CFU of *E. faecium 11236/1*, a full protection in the group immunised with Sc (EH)$_3$ antibodies (0% of mortality) and a significant decrease of mortality in the group immunised with anti-AdcA antibodies (30%) were observed compared to 90% of mortality in the untreated control group ($p < 0.0001$ and $p < 0.05$, respectively). For *E. faecalis* T2 strain, after 96 h of bacterial challenge with 6×10^9 CFUs, no mortality was observed in the mice immunised with either Sc (EH)$_3$ or AdcA antibodies, compared to 60% of mortality in the control group ($p < 0.001$) (Fig. 7B). For *S. aureus MW2*, after 96 h of bacterial challenge with 9×10^9 CFU, a statistically significant decreased mortality was observed in the group immunised with Sc(EH)$_3$ antibodies (20% of mortality) but not significant with anti-AdcA (70% of mortality) compared to 100% mortality in the control group ($p = 0.001$ and $p = 0.06$, respectively).

Active immunisation with Sc(EH)$_3$ and AdcA antigens induces protective antibodies in mouse infection models

To demonstrate that Sc(EH)$_3$ and AdcA antigens stimulate the immune system by inducing protective antibodies, we performed active immunisation with four doses of 10 µg of antigen, as detailed in Supplementary Fig. 5. We first performed a whole bacterial ELISA to quantify the levels of specific IgG antibodies against three Gram positive pathogens (*E. faecium* 11236/1, *S. aureus* MW2 and *E. faecalis* T2) in the sera of mice immunised with Sc(EH)$_3$ and AdcA antigens, after 2 subcutaneous doses and after 2 intraperitoneal doses (Supplementary Fig. 5). Higher levels of antibodies were found both in the sera of mice immunised with Sc(EH)$_3$ and AdcA antigens (Fig. 8A, B, respectively), compared to non-immunised groups, already after the 2 subcutaneous doses. Antibody levels increased after 4 weeks of immunisation, following the two further intraperitoneal injections (Fig. 8A, B). These results show that the both the immunisation with Sc(EH)$_3$ and AdcA antigens induced a strong immune response and triggered the production of antibodies. Then, mice were challenged with intraperitoneal injections of lethal doses (Supplementary Fig. 5) of three tested Gram-positive bacteria.

As shown in Fig. 8C, after 96 h of bacterial challenge with the lethal dose (9×10^9 CFU) of *E. faecium 11236/1*, a significant decrease of mortality

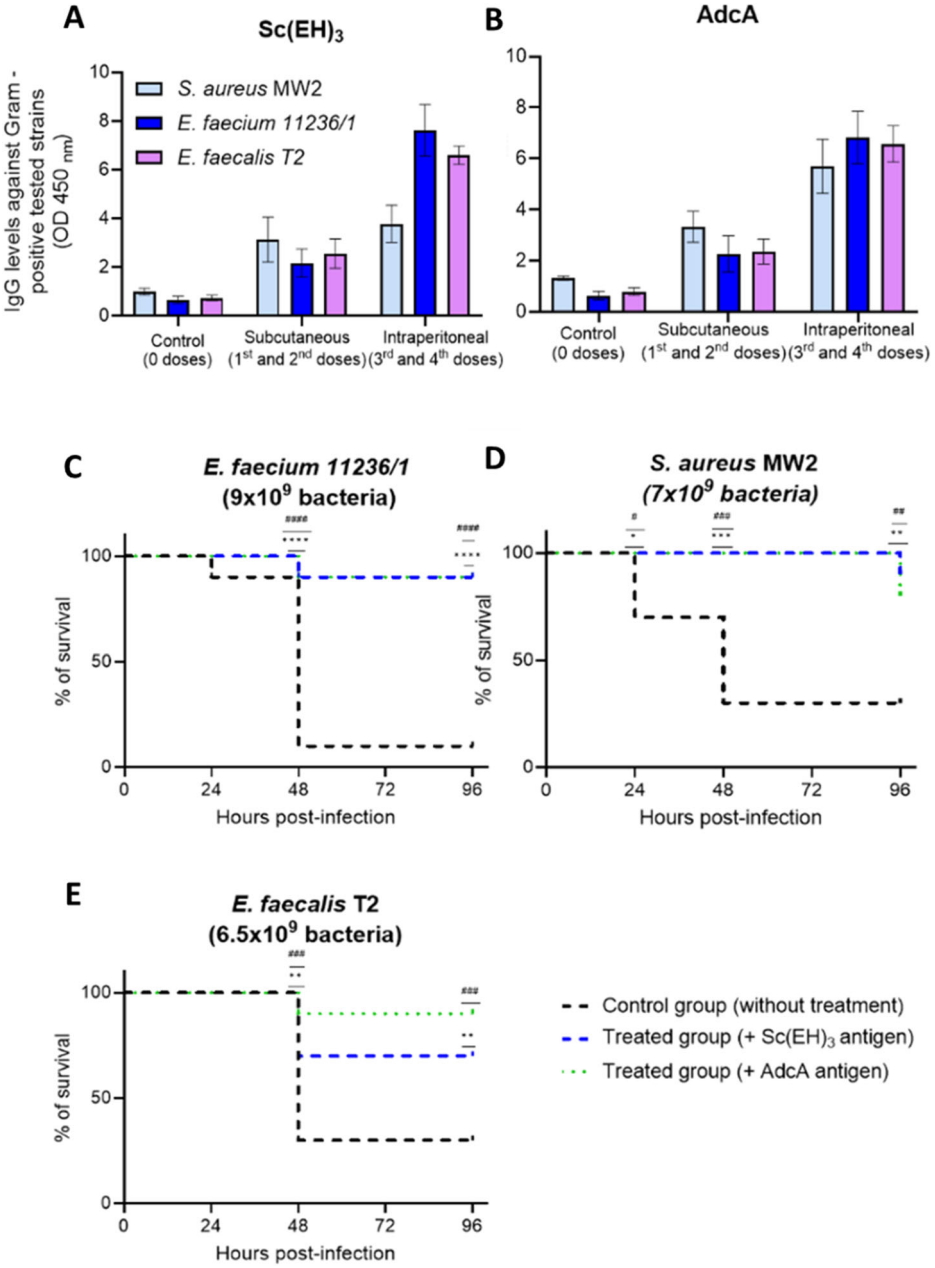

Fig. 8 | In vivo active protective efficacy of $Sc(EH)_3$ and AdcA antigens against *E. faecium*, *E. faecalis* and *S. aureus*. **A** IgG responses of mice immunised with $Sc(EH)_3$ antigen in each group (*S. aureus* MW2, *E. faecium* 11236/1 and *E. faecalis* T2) ($n = 10$ per group), after two subcutaneous doses (after 2 weeks) and two intraperitoneal doses (after 4 weeks), compared to the control group receiving only buffer and IFA ($n = 10$). **B** As in panel (**A**), IgG responses of mice immunised with AdcA antigen+IFA ($n = 10$ per group) compared to the control group ($n = 10$). **C** Percentage of survived mice during the active protection assay against 9×10^9 CFU of *E. faecium* 11236/1, (**D**) against 7×10^9 CFU of *S. aureus* MW2 and (**E**) against 6.5×10^9 CFU of *E. faecalis T2*. The discontinuous blue line represents the group treated with $Sc(EH)_3$ antigen ($n = 10$), the green line the group treated with AdcA antigen ($n = 10$) and the black line the untreated control group ($n = 10$). Statistical differences between groups were assessed using Log Rank (Mantel-cox test). Difference between the treated groups with $Sc(EH)_3$ antigen and the control groups are marked by star symbol, ns: not significant; $^*p < 0.05$, $^{**}p < 0.01$, $^{***}p < 0.001$ and $^{****}p < 0.0001$. Difference between the treated groups with AdcA antigen and the control groups are marked by hash symbol, ns: not significant; # : $p < 0.05$, # # : $p < 0.01$, # # # : $p < 0.001$ and # # # # : $p < 0.0001$.

was observed both in the group immunised with $Sc(EH)_3$ and with AdcA (only 10%), compared to 90% mortality in the untreated control group ($p < 0.0001$). Similarly, after 96 h of challenge with 7×10^9 CFU *S. aureus* MW2, a statistically significant decreased mortality was observed in both groups immunised with $Sc(EH)_3$ (10% mortality) and AdcA (20% mortality), compared to 70% mortality in the untreated control group ($p < 0.001$ both, Fig. 8D). In the case of *E. faecalis* T2 strain, 96 h after the bacterial challenge with the lethal dose (6.5×10^9 CFUs), 30% mortality was observed in the mice immunised with $Sc(EH)_3$ and 10% in mice immunised with AdcA, compared to 70% mortality in the untreated control group ($p < 0.01$ and $p < 0.001$ respectively, Fig. 8E). Overall, these results show that the active immunisation with $Sc(EH)_3$ and with AdcA antigens induce a strong antibody mediated immune response and leads to a significant protection in a lethal bacteremia mouse model.

Discussion

MRSA and VREfm are a serious threat all over the world in hospitals and long-term care units among patients of all ages. Targeted actions are urgently needed to prevent a further acceleration of this problem[11,55]. Although several candidate vaccine antigens have been proposed against *E.faecium*[14–20], and against *S. aureus*[56–59], no vaccines are currently available[22]. Preventing *S. aureus* infection has proven to be challenging, given the high rate of failures in the clinical trial stage[32,60].

In response to this urgent and unmet need for non-antibiotic approaches, we tried to identify vaccine antigens with a potential use against several pathogens, with the idea to design an antigen that would be active against a larger panel of clinically relevant Gram-positive pathogens. Indeed, Pan-vaccinomics approaches are currently an important strategy for the development of universal vaccine candidates against WHO priority pathogens[61]. Starting from our preliminary observation that antibodies raised *E. faecium* AdcA mediate opsono-phagocytosis in *S. aureus* strains expressing all major type of capsules (CP5, CP8 and non-typable strains), we developed a structural vaccinology approach, identifying a region of AdcA, the EH-motif, that was predicted to be highly immunogenic and is also highly conserved among a wide spectrum of Gram-positive pathogens. We subsequently designed a novel molecule with multiple presentation of the

EH-motif, $Sc(EH)_3$, that consists of a rigid core and flexible EH-motifs located in two loops and on the N-terminus of the protein, as shown by MD simulations. Flexibility of antigens is an often-neglected feature that may improve an immunological response. Indeed, multiple potential conformations of a specific antigen seems beneficial as it increases variability of antigenic presentation during recognition by B-cells, which can broaden the diversity of antibodies in the immune response[54]. We could demonstrate in in vitro and in vivo assays that $Sc(EH)_3$ is immunogenic in rabbits, and leads to antibodies that successfully mediate opsonic killing of *E. faecium* 11236/1, *S. aureus* MW2, *E. faecalis* T2.

For nosocomial pathogens, passive immunisation for post-exposure prophylaxis has great advantages, compared to vaccination. Indeed, protection afforded via passive immunisation is immediate, and such protection can be induced in immunosuppressed individuals who are often at the highest risk of infection[62]. With this idea in mind, we demonstrated that anti-$Sc(EH)_3$ antibodies are protective in mice challenged with *E. faecium* 11236/1, *S. aureus* MW2, *E. faecalis* T2. Also, anti-$Sc(EH)_3$ antibodies are significantly more effective than anti-AdcA post-challenge with these bacterial strains. The high conservation of the EH-motif also in *Streptococci*, and the key role of ABC transporter proteins AdcAI and AdcAII for full pathogenic potential in *Streptococcus pneumoniae* and *S. pyogenes*[38,63] suggests promising further applications; however, additional work is needed to understand whether the spectrum of applicability of $Sc(EH)_3$ can be extended to this family.

To extend the applicability of $Sc(EH)_3$ antigen in vaccination, we also performed active immunisation studies and showed that both $Sc(EH)_3$ and AdcA antigens develop a strong immune response in mice, generating protective antibodies against *E. faecium* 11236/1, *E. faecalis* T2 *S. aureus* MW2. In active immunisation, immunogenic performances of $Sc(EH)_3$ were comparable to those of AdcA. Despite this, a strong advantage of $Sc(EH)_3$ over AdcA in active immunisation is its extremely high thermal-stability and resistance to proteolysis for prolonged storage time at 37 °C. Stability of vaccines, especially during transportation, is still a great challenge[64,65], as a large component of vaccination costs arises from maintaining cold chains, storage, and transport rather than the actual cost of vaccine production. In some parts of the world, the WHO–UNICEF Expanded Program on Immunisation has the formidable task to deliver vaccines to the respective populations at risk, investing huge financial and human resources to maintain a cold chain. Providing hyper-thermostable antigen formulations with prolonged expiration date could be of benefit in demanding environments, such as tropical countries[66].

Although vaccines are not solely composed of subunit antigens, we believe that a soluble, highly stable multi-targeting antigen can greatly affect the usage of a final formulation. Moreover, the strategy presented in this paper could be applied to multiple antigens through the identification of their immunogenic epitopes and their use in new vaccine formulations. This may further enhance the coverage and durability of immune responses against these ESKAPE pathogens and reduce the likelihood of immune evasion. Overall, this approach holds promise for developing vaccines with enduring efficacy against diverse strains and serotypes of bacterial pathogens. Taken together, our findings can be seen as a step forward in a field of pan-vaccinomics, that will address all Gram positive AMR pathogens from the pathogens of concern list of the WHO[61]. In conclusion, the EH-motif epitope, particularly in the hyper stable $Sc(EH)_3$ configuration, shows promise as an antigen for developing a vaccine against all Gram-positive ESKAPE pathogens. Our data provide evidence in support of a rational structure-based approach, combining in silico, in vitro, and in vivo experiments, for the identification of specific cross-reactive epitopes and has the potential to enhance vaccine formulations, widening their coverage as well as facilitating the development of broad-spectrum monoclonal antibodies.

Methods details

Bioinformatic analysis

Homology modelling of AdcA from *E. faecium* was obtained using MODELLER[36] after consensus-based sequence alignment using HHpred[37]. The best template was the crystal structure of AdcA from *S. pneumoniae* (PDB:7JJ9, sequence identity 65,33%). AdcA homology model and AdcA sequence were used for epitope predictions, using a panel of the software. Among these, VaxiJen is an artificial intelligence software that was trained on known antigens and properties of amino acids in antigenic proteins[42]. BepiPred2 was used to predict the presence of linear B cell epitopes[67]. BepiPred2 is based on a random forest algorithm trained on epitopes annotated from antibody-antigen protein structures. Discotope was used for structure-based epitope predictions[52]. Almost the same results were obtained using an AdcA model obtained using Artificial Intelligence and the program AlphaFold2.0.

Allergenicity was computed using AllerTOP v2.0[43] and AllergenFP v.1.0[44], which describe amino acids in given sequences using five E-descriptors: hydrophobicity, molecular size, helix-forming propensity, a relative abundance of amino acids, and β-strand forming propensity. Proteins are classified as allergenic or non-allergenic based on the k-nearest neighbour algorithm (kNN, k = 1), to which training a set containing 2427 known allergens from different species and 2427 non-allergens was used. Toxicity of the antigen was computed with ToxinPred[45], a protein scanning tool, based on machine learning techniques and quantitative matrix through the recognition of motifs detected in toxins.

Homology searches were performed using BlastP in the non-redundant protein sequences (nr) database. To improve our search, we used the ZnuA domain of AdcA with a query subrange for peptide G125-H141. Different thresholds were used to obtain primary datasets, which further were uploaded into EMBL-EBI software Clustal Omega[47] and analysed. For multiple sequence alignment visualisation and manipulation, we used Jalview 2[48]. Sequences with additions or deletions in EH rich region were manually removed and subtracted from the dataset used for consensus sequence. Alignment data can be found in the supplementary data.

Design of $Sc(EH)_3$ and molecular dynamics analysis

We used domain D1 of Arginine Binding Protein from *Thermatoga maritima* (TmArgBP) (PDB 6gpc)[49], where we introduced the identified highly antigenic sequence of AdcA, the EH-motif, at specific locations, guided by molecular modelling. This model was used for further computational analysis, using Molecular Dynamics (MD). MD simulations were run with GROMACS 2020.3, in an octahedron box using a TIP3P water model[68]. Ions were added to reach neutrality. Periodic Boundary Conditions were employed and the LINCS algorithm was used to constrain all bond lengths. An integration time step of 2 fs was used. The particle mesh Ewald method was used to treat electrostatics, a non-bonded cut-off was applied for the Lennard-Jones potential. Temperature (T = 300 K) and pressure (p = 1 atm) were controlled using the v-rescale and the Parrinello-Rahman[69] algorithms, respectively. Water molecules were relaxed by energy minimisation and followed by 10 ps MD at 300 K, harmonically restraining the atomic positions. The systems were heated up gradually to 300 K in a six-step process, from 50 K to 300 K. Three short 5 ps-long equilibrations at 300 K at NPT were run changing the velocity seeds and finally, three production simulations were run under NPT conditions without restraints for 500 ns each. The last 400 ns of the three velocity simulations were concatenated excluding the first 100 ns of each to ignore the equilibration phase. The analyses of the trajectories were done with GROMACS, PyMOL[70], and VMD (http://www.ks.uiuc.edu/). The simulation frames were clustered and the structures exhibiting the lowest RMSD relative to the other members of the most populated cluster were selected as MD representatives.

Bacterial strains

E. coli Top10, *E. coli* BL21 (DE3) and *E.coli* Rosetta 2 (DE3) were obtained from collection of Institute of Biostructures and Bioimaging of Italian National Research Council. *E. coli* M15pRep4, *E. faecium* 11236/1, *S. aureus* MW2, *E. faecalis* T2 were obtained from Dr. von Hauner's Children's Hospital.

Antigen production

For production and vector propagation, strains of *Escherichia coli* TOP10 (DE3) and *E.coli* Rosetta 2(DE3) were routinely grown in Luria-Bertani (LB) (1% w/v NaCl, 1% w/v Tryptone, 0.5% w/v Yeast extract (BioFroxx)) broth with shaking and on LB agar solid medium at 37 °C with dedicated antibiotics: kanamycin (*E. coli* TOP10) (DE3) and kanamycin and chloramphenicol for *E.coli* Rosetta 2 (DE3) (Sigma-Aldrich). The synthetic gene of $Sc(EH)_3$ (EUROFINS GENOMICS) was subcloned into the pETM-13 vector (EMBL) using NcoI/XhoI (New England Biolabs) restriction enzymes, adding not removable his-tag on the C-terminus. Vector was introduced via heat shock and multiplied in *Escherichia coli* TOP10 (DE3) and further purified with a QIAprep Spin Miniprep Kit (Qiagen). Production was carried out in *E.coli* Rosetta 2 (DE3) strain. For production, 10 mL of overnight *E. coli* Rosetta 2 (DE3) with $Sc(EH)_3$ plasmid were added to 1 L of LB broth with chloramphenicol and kanamycin. The culture was kept at 37 °C with agitation 180 rpm until OD600 reached 0,8. After this, the culture was induced with 0,2 mM isopropyl β- d-1-thiogalactopyranoside (IPTG) (Sigma-Aldrich) and transferred to 22 °C with agitation 180 rpm for overnight protein production. For harvesting culture was centrifuged for 15 min at 4 °C, at 9110 Relative Centrifugal Force (RCF) (xg). Pellet was dissolved in lysis buffer (300 mM NaCl (BioFroxx), 50 mM Tris-HCl (PanReack AppliChem), 2,5% (v/v) glycerol (PanReack AppliChem), pH 7,4) containing protease inhibitor cocktail (Roche) and further sonicated on ice for 15 min (10-sec sonication followed by 10-sec rest). Solution centrifuged at 4 °C for 45 min, 24905 RCF (xg). The supernatant was transferred onto the Ni-NTA agarose (Thermo Scientific™) column, where washing steps were performed with buffer A (300 mM NaCl, 50 mM Tris-HCl, 2.5% (v/v) glycerol, pH 7.4). Elution of the protein was performed at a final concentration of 200 mM imidazole (Sigma-Aldrich) and concentrated on amicons 10k Da cut-off (Merck Millipore). Then, $Sc(EH)_3$ was loaded on Superdex 200 increase 10/300 GL (Cytiva) pre-equilibrated in a buffer containing 50 mM Tris-HCl, NaCl 150 mM, and 5% (v/v) glycerol, pH 7.4. Protein was re-concentrated on amicons 10 kDa cut-off (Merck-Millipore). For protein quantification, we used the Bradford reaction with a ready-to-use reagent Bradford - Solution for Protein Determination (PanReac AppliChem) according to manufacturer instructions.

The AdcA gene (EFF33485) was amplified excluding the sequence corresponding to the signal peptide using the primers AdcA-5-BamHI aggcGGATCCTCGAATGATAAAGATGGAAAAT and AdcA-3-PstI aggcCTGCAGTTAATGAGCCATCATTTCTTGA and digested with corresponding restriction enzymes BamHI/PstI (New England Biolabs). Further, amplicons were inserted downstream of the IPTG-inducible promoter into the pQE30 expression vector (QIA expressionist kit; Qiagen). The resulting construct was heat-shock-transferred into the *E. coli* TOP10 (DE3) and *E. coli* BL21 (DE3). Production and purification followed the same procedure as for the $Sc(EH)_3$. The ZnuA gene was amplified excluding the sequence corresponding to the signal peptide, with primers actacGGATCCAAATTAGAAATTGTAACAAC and gactagAAGCTTAAACCATAGTTGTTTTTTCTAACGC. The amplicons where then digested with corresponding restriction enzymes and inserted downstream of the IPTG-inducible promoter into the pQE30 expression vector to obtain an N-terminal His6-tagged recombinant protein. The resulting construct was electroporated into *E. coli* M15pRep4. Recombinant protein was overproduced in LB buffer and purified under denaturing conditions using the Protino Ni-NTA Agarose (Macherey-Nagel) resin, following the manufactures instructions. Finally, the purified protein was desalted by diafiltration using the Amicon Ultra-15 Centrifugal Filter Units of 3KDa (Merck-Millipore). For immunisation protocols all proteins were dialysed to a buffer composed of 150 mM NaCl, 50 mM Tris 7.8, and 2.5% (v/v) glycerol.

Circular dichroism spectroscopy

Circular dichroism (CD) spectra were measured using a Jasco J-810 spectropolarimeter with a Peltier temperature control system (Model PTC-423-S, Jasco Europe, Cremella (LC), Italy). Far-UV measurements at a protein concentration of 0.2 g/L were carried out in 10 mM phosphate buffer, after 1 h incubation at 20 °C, 37 °C and 100 °C, using a 0.1 cm optical path length cell. The range of the reported wavelengths 196–260 nm was fine-tuned as a function of the observed HT voltage. The spectra, recorded with a time constant of 4 s, a 2 nm bandwidth, and a scan rate of 10 nm min^{-1}, were signal averaged over at least two scans. The final spectra were expressed as molar ellipticity [θ] (deg cm^2dmol^{-1}) *per* residue. The temperature of the transition midpoint (T_d) was investigated by monitoring the change in ellipticity at 222 nm while increasing the temperature from 20 °C to 100 °C. To facilitate denaturation 3 M GuHCl (Sigma-Aldrich) was added. The reversibility of the transition was checked by lowering the temperature to 20 °C and re-scanning the sample without the denaturation agent. The curve was registered using a 0.1 cm path length cell, a protein concentration of 0.2 g/L, and a scan rate of 1.0 °C min^{-1}. Data were analysed using the origin software (OriginLab).

Light scattering studies

Purified protein was analysed by size-exclusion chromatography connected to a triple-angle light scattering detector equipped with a QELS module (quasi-elastic light scattering). Protein samples of 500 µg were loaded on a Superdex 200 increase 10/300 GL (Cityvia) column, equilibrated in 50 mM Tris-HCl, 150 mM NaCl, 5% (v/v) glycerol, pH 7,4. A flow rate of 0.5 mL/min was applied. Elution profiles were detected by a Shodex interferometric refractometer and analysed using a miniDawn TREOS light scattering system (Wyatt Instrument Technology Corp.). Data processing was carried out using the Astra 5.3.4.14 software package.

Production of rabbit polyclonal sera

The immunisation protocol with the $Sc(EH)_3$ antigen was carried out by the company Biogenes GmbH (Berlin, Germany) following national and international animal welfare regulations for housing, immunizing, and collecting serum samples from rabbits. The protocols were approved by the National Institutes of Health Office of Laboratory Animal Welfare (identifier A5755-0) and were performed as follows: Two female New Zealand white rabbits (Biogenes GmbH, Berlin, Germany) with low pre-existing antibodies against enterococcus and staphylococcus were selected before starting the immunisations, 10 mL of sera from each animal were collected to be used as negative controls. An initial immunisation was performed via intramuscular injection (i.m.) with 73.2 nM of protein without any adjuvant. Three i.m. boosts were performed two, four and six weeks after the initial immunisation with 14.6 nM of protein without any adjuvant. To ensure good immunogenicity, one final boost was given to the rabbits on week eight using 14.6 nM of protein combined with a proprietary adjuvant from the company Biogenes, administered through the same route as previous injections. The terminal bleeding was collected in the tenth week. All collected sera were heat-inactivated at 56 °C for 30 min. Before being used, sera were frozen and kept at −20 °C. For OPKA and OPIA assays sera from the same time points were mixed 1:1 to have the average immune response of the rabbits. Anti-AdcA polyclonal serum was collected before as described elsewhere[18] and further stored in aliquots at −20 °C and thawed when needed.

IgG quantification

The concentration of IgG antibodies was determined using the sandwich ELISA method[71]. Plates were coated overnight with anti-rabbit IgG (Abcam) at 1 µg/mL concentration in 0.2 M sodium carbonate(Sigma-Aldrich)/bicarbonate (Sigma-Aldrich) buffer, pH 9.4 and kept at 4 °C. Blocking was carried out using 3% BSA in PBS (Sigma-Aldrich) solution for 1 h at RT. Investigated sera and rabbit IgG used for calibration curve were diluted in 1% BSA, 0.5% Tween20, PBS solution and incubated on the plate for 2 h at RT. All the steps were separated by washing three times each well with 0.9% NaCl solution with 0.1% Tween20. For detection, we used disodium p-nitrophenyl phosphate at final concentration 1 mg/mL in 0.1 M glycine buffer with 1 mM $MgCl_2$ and 1 mM $ZnCl_2$ (all powders were from PanReac AppliChem), pH 10.4. Incubation in the dark was performed for

30 min after which the reaction was stopped by adding 3 M NaOH. Absorbance was measured at 405 nm wavelength using microplate absorbance spectrophotometer (Bio-Rad) and IgG concentration was calculated using an IgG calibration curve.

Immunoreactivity of the EH-motif tested by ELISA

Either anti-AdcA or anti-Sc(EH)$_3$ rabbit serum specificity against the different biotinylated peptides (i.e. C-biot-EH and N-biot-EH) was tested by ELISA using high-capacity streptavidin-coated plates (Thermo Scientific™) as described elsewhere[72]. Briefly, wells were washed three times with 200 µL of tween-BSA buffer (TBT: 1× Tris-buffered saline (TBS) (PanReac AppliChem), 0.1% BSA (Sigma-Aldrich), and 0.05% Tween20 (Sigma-Aldrich)). Then, the plates were coated with 0.5 µg of the corresponding antigen dissolved in TBT per well and incubated for 2 h at 4 °C. Wells were washed as described above. Then, 100 µL of anti-rabbit serum in triplicate for each dilution (ranging between 1:250 to 1:160,000) were added to the plates and incubated for 2 h at RT with gentle shaking. Again, wells were washed three as described above and incubated for 60 min at RT with a 100 µL of alkaline-phosphatase-conjugated anti-rabbit IgG produced in goats (Invitrogen™) at a 1:1000 dilution. Finally, wells were washed four times with 200 µL of TBT, and 100 µL of p-nitro phenyl phosphate (Sigma-Aldrich) at 1 mg/mL in glycine buffer (PanReac AppliChem) was added to each well as the substrate. Plates were incubated at RT in the dark for 60 min for colour development. The reaction was then stopped by adding 50 µL of 3 M sodium hydroxide, and the absorbance was measured at 405 nm.

Opsonophagocytic killing assay and opsonophagocytic inhibition assay

For OPKA and OPIA assays, we used *E. faecium* 11236/1, *S. aureus* MW2 and *E. faecalis* Type 2, which were grown in tryptic soy agar (TSA) (Thermo Scientific™) and broth (TSB) (Thermo Scientific™) at 37 °C. The enterococcal strains were cultivated without agitation whereas the *S. aureus* strains were grown with agitation.

OPKA and OPIA are widely used to present opsonophagocytic-dependent bacteria-killing with the usage of chosen agent and the specificity of this action. Full protocols of both assays were previously described elsewhere[16]. Shortly, four components were prepared: (a) baby rabbit complement (Bio-Rad) absorbed with the target bacterial strain as a source of complement, (b) rabbit sera before and after immunisation with the different antigens (c) polymorphonuclear neutrophils (PMNs) freshly prepared from human blood collected from healthy adult volunteers, and (d) the bacterial strains grown to OD650 nm = 0.4 in tryptic soy broth (TSB). For the OPKA, the four components were mixed: 100 µL of PMNs ($2.5 \times 10^4\,\mu L^{-1}$); 100 µL of the appropriate serum concentration, 100 µL of complement (1 : 15 dilutions for the enterococcal strains, and 1 : 30 for *S. aureus* strains), and 100 µL of an appropriate dilution of bacteria. All the needed dilutions were made with RPMI 1640 (Gibco) + 15% foetal bovine serum (FBS) (Gibco) (RPMI-F). The mixture was incubated on a rotor rack at 37 °C for 90 min, after this time samples were diluted in TSB, and plated on TSA plates in quadruplicate. The percentage of killing was calculated by comparing the colony counts at 90 min of a control (no PMNs) to the colony counts of a tube that contained all four components of the assay using the following formula:

$$\%\text{Killing} = \{[(\text{mean CFU control at 90 min}) - (\text{mean CFU at 90 min})]/(\text{mean CFU control at 90 min}) \times 100\%\}$$

The same protocol was used for OPIA experiments, with the difference that sera were diluted to the final concentration of 0.4 mg/mL and pre-incubated overnight at 4 °C with an equal volume of RPMI-F with the epitope carrying proteins (inhibitors). Inhibition assays were performed at serum dilutions yielding 50–60% killing of the inoculum. We compared the percentage of inhibition of opsonophagocytic killing to controls without inhibitors. For the controls we used (i) bacteria incubated in RPMI-F, (ii) bacteria incubated in RPMI-F with complement at the corresponding dilution, (iii) bacteria incubated in RPMI-F with PMN's, and (iv) bacteria incubated in RPMI with complement and PMN's. As a positive control in OPIA, we used sera raised against AdcA. To show that the response is immunisation dependent and to exclude minimal natural response in rabbits, sera collected before antigen administration were used as negative controls.

Ethical statement for animal experimentation

Six weeks old female BALB/cJRJ were obtained from Janvier Labs (Janvier Laboratories, Lyon, Saint Berthevin, France) and were housed in a controlled temperature and pressure environment at the Imagine Institute-SFR Necker (Paris, France). Mice were adapted to new environmental conditions for one week before the experimental procedure started. The animals were house kept in cages with water and food ad libitum enriched with cardboard house with cotton squares for nests. The experimental protocol was approved by the animal Experimentation Ethics Committee under reference number 202201311143868 and all animals handling and procedures were performed in accordance with the French Decree N° 2013–118, 7 February 2013 and with European law in agreement with animal research.

Median lethal dose determination

Before the immunisation, a pilot study was performed to determine the challenge bacterial dose. An approximate LD50 was estimated using five different mice group (3- 4 mice per group for *E. faecium* 11236/1 and *E. faecalis* T2 and 4–5 mice per group for *S. aureus* MW2) per each bacterial strain with increased dose of bacteria ranging from 10^8 to 10^{10} CFU/ml of fresh bacterial culture in stationary phase (OD = 1) The mice received the different bacterial doses by intraperitoneal (i.p) injection. Mice were monitored for one week end the mortality rate in each group was determined (Supplementary Table 2). At the end of the experiment, all animals were euthanised by cervical dislocation.

Passive immunization

Six weeks old female BALB/cJRJ were passively immunised intraperitoneally with 200 µl of 50 µg of polyclonal anti-Sc (EH)$_3$ or anti-AdcA sera 24 and 4 h prior the bacterial challenge and 4 h after the bacterial challenge. A heat inactivated Baby Rabbit Complement (BRC) (Cedarlane laboratories, Canada) was used as a negative control ($n = 10$ for each bacterial strain used). Mice were challenged intraperitoneally with approximately 8×10^9 CFUs of *E. faecium* 11236/1 ($n = 10$), 6×10^9 CFUs of *E. faecalis* T2 ($n = 10$) or 9×10^9 CFUs of *S. aureus* MW2 ($n = 10$). Mice were followed for 96 h post-infection and the mortality rate was recorded per group. Also, when mice became moribund, as defined by hunched appearance, markedly increased respiration rate, piloerection, and lack of an ability to move in response to being touched, they were euthanised and counted as dead for these experimental outcomes. In the end of experiment, surviving mice were euthanised by cervical dislocation (Supplementary Fig. 4).

Active immunization

Six weeks old female BALB were injected subcutaneously with 10 µg of Sc (EH)$_3$ or AdcA antigen emulsified in 100 µl complete Freud's adjuvant. Seven days post vaccination, mice were boosted subcutaneously with 10 µg of Sc (EH)$_3$ or AdcA antigen emulsified in 100 µl incomplete Freud's adjuvant. Mice were then boosted intraperitoneally with 10 µg of Sc(EH)$_3$ or AdcA antigen suspended in saline on days 14 and 21. A negative control group was included with mice receiving only saline each time antigen is injected. A blood sample was collected at 13 and 21 days to evaluate the levels of antibodies developed by the immunised mice Then, mice were challenged intraperitoneally seven days after the final boost with approximately 9×10^9 CFUs of *E. faecium* 11236/1 ($n = 10$), 6.5×10^9 CFUs of *E. faecalis* T2 ($n = 10$) or 7×10^9 CFUs of *S. aureus MW2* ($n = 10$). Mice were followed for 96 h post-infection and the mortality rate was recorded per group (Supplementary Fig. 5).

Antibody response of immunised mice

To assess the antibodies titre in the immunised mice, we performed a whole-bacterial-cell ELISA as previously described[73]. To obtain heat-stable antigens from the various strains, bacteria were inactivated for 60 min in a water bath at 70 °C after an overnight culture in Tryptic Soy Broth (TSB) liquid at 37 °C. The culture media were centrifuged at 20,000 × *g* for 10 min. The pellets were resuspended in PBS and diluted to an OD_{600} of 0.1. Next, 100 µl of the different bacterial suspension were coated onto 96-well ELISA plates, which were incubated overnight at 37 °C. On the next day, 100 µl of bovine serum albumin (BSA) 1% were added to each well and incubated for 90 min at 37 °C. After washing with a mixture of PBS and Tween® 20 (Sigma-Aldrich, St. Louis, MO, USA), 100 µL of mice sera were added to each well and incubated for 2 h at 37 °C. Next, 100 µL of a 1:10,000 dilution of anti-mouse secondary antibodies (rabbit anti-mouse IgG H&L, Sigma-Aldrich) coupled to horseradish peroxidase were added. A substrate was then used to reveal the reaction (TMB Liquid Substrate, Sigma-Aldrich) by spectrophotometry.

Quantification and statistical *analysis*

In vitro data were analysed using Prism 7 (GraphPad Software, La Jolla, CA). Plots show mean ± SEM. ($^{*}P \le 0.05$, $^{**}P \le 0.01$, $^{***}P \le 0.001$). Animal model data were analysed using Prism 9.2 (GraphPad Software, La Jolla, CA). The results were expressed as mean ± SD.

Data availability

Additional data that support the findings of this study, are available in the Supplementary material. Further information and requests for resources and reagents should be directed to and will be fulfilled by the lead contacts (rita.berisio@cnr.it).

Received: 28 December 2023; Accepted: 30 July 2024;
Published online: 18 August 2024

References

1. Wan, L. Y. M., Chen, Z. J., Shah, N. P. & El-Nezami, H. Modulation of intestinal epithelial defense responses by probiotic bacteria. *Crit. Rev. Food Sci. Nutr.* **56**, 2628–2641 (2016).
2. Krawczyk, B., Wityk, P., Gałęcka, M. & Michalik, M. The many faces of enterococcus spp.—Commensal, probiotic and opportunistic pathogen. *Microorganisms* **9**, 1900 (2021).
3. Lebreton, F., Willems, R. J. L. & Gilmore, M. S. Enterococcus Diversity, Origins in Nature, and Gut Colonization. In Enterococci: From Commensals to Leading Causes of *Drug Resistant Infection* (eds. Gilmore, M. S., Clewell, D. B., Ike, Y. & Shankar, N.) (Massachusetts Eye and Ear Infirmary, Boston, 2014)
4. Weiner, L. M. et al. Antimicrobial-resistant pathogens associated with healthcare-associated infections: summary of data reported to the national healthcare safety network at the centers for disease control and prevention, 2011–2014. *Infect. Control Hosp. Epidemiol.* **37**, 1288–1301 (2016).
5. Zhou, X., Willems, R. J. L., Friedrich, A. W., Rossen, J. W. A. & Bathoorn, E. Enterococcus faecium: From microbiological insights to practical recommendations for infection control and diagnostics. *Antimicrob. Resist. Infect. Control* **9**, 130 (2020).
6. Kodali, S. et al. A vaccine approach for the prevention of infections by multidrug-resistant Enterococcus. *faecium. J. Biol. Chem.* **290**, 19512–19526 (2015).
7. Chilambi, G. S. et al. Evolution of vancomycin-resistant Enterococcus faecium during colonization and infection in immunocompromised pediatric patients. *Proc. Natl. Acad. Sci. USA* **117**, 11703–11714 (2020).
8. Jabbari Shiadeh, S. M., Pormohammad, A., Hashemi, A. & Lak, P. Global prevalence of antibiotic resistance in blood-isolated Enterococcus faecalis and Enterococcus faecium: a systematic review and meta-analysis. *Infect. Drug Resist.* **12**, 2713–2725 (2019).
9. Ch'ng, J.-H., Chong, K. K. L., Lam, L. N., Wong, J. J. & Kline, K. A. Biofilm-associated infection by enterococci. *Nat. Rev. Microbiol.* **17**, 82–94 (2019).
10. Ben Braïek, O. & Smaoui, S. Enterococci: Between emerging pathogens and potential probiotics. *BioMed Res. Int.* **2019**, e5938210 (2019).
11. Tacconelli, E. et al. Discovery, research, and development of new antibiotics: The WHO priority list of antibiotic-resistant bacteria and tuberculosis. *Lancet Infect. Dis.* **18**, 318–327 (2018).
12. Murray, C. J. I. et al. Global burden of bacterial antimicrobial resistance in 2019: a systematic analysis. *Lancet Lond. Engl.* **399**, 629–655 (2022).
13. Vekemans, J. et al. Leveraging Vaccines to Reduce Antibiotic Use and Prevent Antimicrobial Resistance: A World Health Organization Action Framework. *Clin. Infect. Dis. Off. Publ. Infect. Dis. Soc. Am.* **73**, e1011–e1017 (2021).
14. Kalfopoulou, E. & Huebner, J. Advances and prospects in vaccine development against Enterococci. *Cells* **9**, 2397 (2020).
15. Kazemian, H. et al. Molecular cloning and immunogenicity evaluation of PpiC, GelE, and VS87_01105 proteins of enterococcus faecalis as vaccine candidates. *Iran. Biomed. J.* **23**, 344–353 (2019).
16. Kropec, A. et al. Identification of SagA as a novel vaccine target for the prevention of Enterococcus faecium infections. *Microbiol. Read. Engl.* **157**, 3429–3434 (2011).
17. Nallapareddy, S. R., Singh, K. V., Sillanpää, J., Zhao, M. & Murray, B. E. Relative contributions of Ebp Pili and the collagen adhesin ace to host extracellular matrix protein adherence and experimental urinary tract infection by Enterococcus faecalis OG1RF. *Infect. Immun.* **79**, 2901–2910 (2011).
18. Romero-Saavedra, F. et al. Characterization of two metal binding lipoproteins as vaccine candidates for enterococcal infections. *PLoS ONE* **10**, e0136625 (2015).
19. Romero-Saavedra, F. et al. Identification of peptidoglycan-associated proteins as vaccine candidates for enterococcal infections. *PLOS ONE* **9**, e111880 (2014).
20. Theilacker, C. et al. Protection against staphylococcus aureus by antibody to the polyglycerolphosphate backbone of heterologous lipoteichoic acid. *J. Infect. Dis.* **205**, 1076–1085 (2012).
21. World Health Organization. Bacterial vaccines in clinical and preclinical development 2021. https://www.who.int/publications-detail-redirect/9789240052451 (2022).
22. Bacterial Vaccines in Clinical and Preclinical Development: An Overview and Analysis. Geneva: World Health Organization; 2022. Licence: CC BY-NC-SA 3.0 IGO.
23. Capdevila, D. A., Wang, J. & Giedroc, D. P. Bacterial strategies to maintain zinc metallostasis at the host-pathogen interface. *J. Biol. Chem.* **291**, 20858–20868 (2016).
24. Xia, P. et al. Zinc is an important inter-kingdom signal between the host and microbe. *Vet. Res.* **52**, 39 (2021).
25. Gao, H., Dai, W., Zhao, L., Min, J. & Wang, F. The role of zinc and zinc homeostasis in macrophage function. *J. Immunol. Res.* **2018**, 6872621 (2018).
26. Grim, K. P. et al. The metallophore staphylopine enables staphylococcus aureus to compete with the host for zinc and overcome nutritional immunity. *mBio* **8**, e01281-17 (2017).
27. Makthal, N. et al. Group A streptococcus adcr regulon participates in bacterial defense against host-mediated zinc sequestration and contributes to virulence. *Infect. Immun.* **88**, e00097–20 (2020).
28. Bayle, L. et al. Zinc uptake by Streptococcus pneumoniae depends on both AdcA and AdcAII and is essential for normal bacterial morphology and virulence. *Mol. Microbiol.* **82**, 904–916 (2011).
29. Burcham, L. R. et al. Identification of zinc-dependent mechanisms used by group B streptococcus to overcome calprotectin-mediated stress. *mBio* **11**, e02302-20 (2020).
30. Lam, L. N., Brunson, D. N., Molina, J. J., Flores-Mireles, A. L. & Lemos, J. A. The AdcACB/AdcAII system is essential for zinc homeostasis and

an important contributor of Enterococcus faecalis virulence. *Virulence* **13**, 592–608 (2022).
31. Salazar, N. et al. The C-terminal domain of staphylococcus aureus Zinc transport protein AdcA binds plasminogen and factor H in vitro. *Pathog. Basel Switz.* **11**, 240 (2022).
32. Proctor, R. A. development of a staphylococcus aureus vaccine: An ongoing journey. *Clin. Infect. Dis. Off. Publ. Infect. Dis. Soc. Am.* **77**, 321–322 (2023).
33. Frost, I. et al. The role of bacterial vaccines in the fight against antimicrobial resistance: an analysis of the preclinical and clinical development pipeline. *Lancet Microbe* **4**, e113–e125 (2023).
34. Rausch, M. et al. Coordination of capsule assembly and cell wall biosynthesis in Staphylococcus aureus. *Nat. Commun.* **10**, 1404 (2019).
35. Mistry, J. et al. Pfam: The protein families database in 2021. *Nucleic Acids Res* **49**, D412–D419 (2021).
36. Webb, B. & Sali, A. Protein structure modeling with MODELLER. *Methods Mol. Biol. Clifton NJ* **2199**, 239–255 (2021).
37. Söding, J., Biegert, A. & Lupas, A. N. The HHpred interactive server for protein homology detection and structure prediction. *Nucleic Acids Res*. **33**, W244–W248 (2005).
38. Luo, Z. et al. A Trap-Door Mechanism for Zinc Acquisition by Streptococcus pneumoniae AdcA. *mBio* https://doi.org/10.1128/mBio.01958-20 (2021).
39. Larsen, J. E. P., Lund, O. & Nielsen, M. Improved method for predicting linear B-cell epitopes. *Immunome Res*. **2**, 2 (2006).
40. Kringelum, J. V., Lundegaard, C., Lund, O. & Nielsen, M. Reliable B cell epitope predictions: Impacts of method development and improved benchmarking. *PLoS Comput. Biol.* **8**, e1002829 (2012).
41. Ponomarenko, J. et al. ElliPro: a new structure-based tool for the prediction of antibody epitopes. *BMC Bioinformatics* **9**, 514 (2008).
42. Doytchinova, I. A. & Flower, D. R. VaxiJen: a server for prediction of protective antigens, tumour antigens and subunit vaccines. *BMC Bioinformatics* **8**, 4 (2007).
43. Dimitrov, I., Flower, D. R. & Doytchinova, I. AllerTOP - a server for in silico prediction of allergens. *BMC Bioinformatics* **14**, S4 (2013).
44. Dimitrov, I., Naneva, L., Doytchinova, I. & Bangov, I. AllergenFP: Allergenicity prediction by descriptor fingerprints. *Bioinformatics* **30**, 846–851 (2014).
45. Gupta, S. et al. In silico approach for predicting toxicity of peptides and proteins. *PLoS ONE* **8**, e73957 (2013).
46. Madden, T. The BLAST Sequence Analysis Tool. The NCBI Handbook [Internet] (National Center for Biotechnology Information (US), 2003)
47. McWilliam, H. et al. Analysis Tool Web Services from the EMBL-EBI. *Nucleic Acids Res.* **41**, W597–W600 (2013).
48. Waterhouse, A. M., Procter, J. B., Martin, D. M. A., Clamp, M. & Barton, G. J. Jalview Version 2—a multiple sequence alignment editor and analysis workbench. *Bioinformatics* **25**, 1189–1191 (2009).
49. Ruggiero, A. et al. A loose domain swapping organization confers a remarkable stability to the dimeric structure of the arginine binding protein from thermotoga maritima. *PLoS ONE* **9**, e96560 (2014).
50. Smaldone, G. et al. Domain communication in thermotoga maritima arginine binding protein unraveled through protein dissection. *Int. J. Biol. Macromol.* **119**, 758–769 (2018).
51. Abraham, M. J. et al. GROMACS: High performance molecular simulations through multi-level parallelism from laptops to supercomputers. *SoftwareX* **1–2**, 19–25 (2015).
52. Haste Andersen, P., Nielsen, M. & Lund, O. Prediction of residues in discontinuous B-cell epitopes using protein 3D structures. *Protein Sci. Publ. Protein Soc.* **15**, 2558–2567 (2006).
53. Kurniawan, J. & Ishida, T. Protein model quality estimation using molecular dynamics simulation. *ACS Omega* **7**, 24274–24281 (2022).
54. Fedechkin, S. O. et al. Conformational flexibility in respiratory syncytial virus G neutralizing epitopes. *J. Virol.* **94**, e01879-19 (2020).
55. Centers for Disease Control and Prevention (U.S.). Antibiotic Resistance Threats in the United States, 2019. https://stacks.cdc.gov/view/cdc/82532, https://doi.org/10.15620/cdc:82532 (2019).
56. Clegg, J. et al. Staphylococcus aureus vaccine research and development: The past, present and future, including novel therapeutic strategies. *Front. Immunol.* **12**, 705360 (2021).
57. Fattom, A. et al. Efficacy profile of a bivalent Staphylococcus aureus glycoconjugated vaccine in adults on hemodialysis: Phase III randomized study. *Hum. Vaccines Immunother.* **11**, 632–641 (2015).
58. Jahantigh, H. R. et al. The Candidate Antigens to Achieving an Effective Vaccine against Staphylococcus aureus. *Vaccines* **10**, 199 (2022).
59. Turner, N. A. et al. Methicillin-resistant Staphylococcus aureus: an overview of basic and clinical research. *Nat. Rev. Microbiol.* **17**, 203–218 (2019).
60. Miller, L. S., Fowler, V. G. Jr, Shukla, S. K., Rose, W. E. & Proctor, R. A. Development of a vaccine against Staphylococcus aureus invasive infections: Evidence based on human immunity, genetics and bacterial evasion mechanisms. *FEMS Microbiol. Rev.* **44**, 123–153 (2020).
61. Ismail, S. et al. Pan-vaccinomics approach towards a universal vaccine candidate against WHO priority pathogens to address growing global antibiotic resistance. *Comput. Biol. Med.* **136**, 104705 (2021).
62. Whaley, K. J. & Zeitlin, L. Emerging antibody-based products for infectious diseases: Planning for metric ton manufacturing. *Hum. Vaccines Immunother.* **18**, 1930847 (2022).
63. Ong, C.-L. Y., Berking, O., Walker, M. J. & McEwan, A. G. New insights into the role of zinc acquisition and zinc tolerance in group A streptococcal infection. *Infect. Immun.* **86**, e00048–18 (2018).
64. Brandau, D., Jones, L., Wiethoff, C., Rexroad, J. & Middaugh, C. Thermal stability of vaccines. *J. Pharm. Sci.* **92**, 218–231 (2003).
65. Pambudi, N. A., Sarifudin, A., Gandidi, I. M. & Romadhon, R. Vaccine cold chain management and cold storage technology to address the challenges of vaccination programs. *Energy Rep*. **8**, 955–972 (2022).
66. Bulula, N., Mwiru, D. P., Swalehe, O. & Thomas Mori, A. Vaccine storage and distribution between expanded program on immunization and medical store department in Tanzania: a cost-minimization analysis. *Vaccine* **38**, 8130–8135 (2020).
67. Jespersen, M. C., Peters, B., Nielsen, M. & Marcatili, P. BepiPred-2.0: Improving sequence-based B-cell epitope prediction using conformational epitopes. *Nucleic Acids Res*. **45**, W24–W29 (2017).
68. Van Der Spoel, D. et al. GROMACS: Fast, flexible, and free. *J. Comput. Chem.* **26**, 1701–1718 (2005).
69. Parrinello, M. & Rahman, A. Polymorphic transitions in single crystals: A new molecular dynamics method. *J. Appl. Phys.* **52**, 7182–7190 (1981).
70. The PyMOL Molecular Graphics System, Version 1.2r3pre. Schrödinger, LLC. (2010)
71. Salauze, D., Serre, V. & Perrin, C. Quantification of total IgM and IgG levels in rat sera by a sandwich ELISA technique. *Comp. Haematol. Int.* **4**, 30–33 (1994).
72. Laverde, D. et al. Synthetic oligomers mimicking capsular polysaccharide diheteroglycan are potential vaccine candidates against encapsulated enterococcal infections. *ACS Infect. Dis.* **6**, 1816–1826 (2020).
73. Sereme, Y. et al. A live attenuated vaccine to prevent severe neonatal Escherichia coli K1 infections. *Nat. Commun.* **15**, 3021 (2024).

Acknowledgements

We would like to acknowledge the support of Michał Krzemieniewski. Funding was provided by the project INF-ACT “One Health Basic and Translational Research Actions addressing Unmet Needs on Emerging Infectious Diseases PE00000007”, PNRR Mission 4, EU “NextGen-eratio-nEU”- D.D. MUR Prot.n. 0001554 of 11/10/2022. E.K. and O.S. were funded

by BactiVax - Anti-Bacterial Innovative Vaccines, Marie Skłodowska-Curie Actions, GA 860325.

Author contributions

R.B., D.S. and F.R. designed the research. E.K. and R.B. carried out bioinformatics analyses. E.K., V.N. and F.S. performed the expression and purification of the $Sc(EH)_3$ antigen and its biophysical characterisation. E.K. and D.L. performed the expression and purification of the AdcA protein and ZnuA domain. E.K., F.R., D.L. and O.S. designed and performed in vitro immunological assays. I.A. performed MD studies. D.S., E.F. and E.T. designed and performed mice model studies. R.B., E.K., J.H. and F.R. analysed the data and prepared the manuscript with input from all authors.

Competing interests

The authors declare no competing interests.

Additional information

Supplementary information The online version contains supplementary material available at https://doi.org/10.1038/s41541-024-00940-x.

Correspondence and requests for materials should be addressed to David Skurnik, Felipe Romero-Saavedra or Rita Berisio.